

# Offsite Evaluation of Localization Systems: Criteria, Systems, and Results From IPIN 2021 and 2022 Competitions

Francesco Potorti <sup>id</sup>, *Senior Member, IEEE*, Antonino Crivello <sup>id</sup>, Soyeon Lee <sup>id</sup>, Blagovest Vladimirov <sup>id</sup>, Sangjoon Park <sup>id</sup>, Yushi Chen <sup>id</sup>, Long Wang <sup>id</sup>, Runze Chen <sup>id</sup>, *Graduate Student Member, IEEE*, Fang Zhao <sup>id</sup>, *Member, IEEE*, Yue Zhuge <sup>id</sup>, Haiyong Luo <sup>id</sup>, *Member, IEEE*, Antoni Perez-Navarro <sup>id</sup>, *Member, IEEE*, Antonio R. Jiménez <sup>id</sup>, Han Wang <sup>id</sup>, *Member, IEEE*, Hengyi Liang <sup>id</sup>, *Member, IEEE*, Cedric De Cock <sup>id</sup>, David Plets <sup>id</sup>, *Member, IEEE*, Yan Cui <sup>id</sup>, Zhi Xiong <sup>id</sup>, Xiaodong Li <sup>id</sup>, Yiming Ding <sup>id</sup>, Fernando Javier Álvarez Franco <sup>id</sup>, *Senior Member, IEEE*, Fernando Jesús Aranda Polo <sup>id</sup>, *Student Member, IEEE*, Felipe Parralejo Rodríguez <sup>id</sup>, *Student Member, IEEE*, Adriano Moreira <sup>id</sup>, *Senior Member, IEEE*, Cristiano Pendão <sup>id</sup>, Ivo Silva <sup>id</sup>, Miguel Ortiz <sup>id</sup>, Ni Zhu <sup>id</sup>, *Member, IEEE*, Ziyou Li <sup>id</sup>, Valérie Renaudin <sup>id</sup>, *Member, IEEE*, Dongyan Wei <sup>id</sup>, Xinchun Ji, Wenchao Zhang <sup>id</sup>, Yan Wang <sup>id</sup>, Longyang Ding <sup>id</sup>, Jian Kuang <sup>id</sup>, Xiaobing Zhang <sup>id</sup>, Zhi Dou <sup>id</sup>, Chaoqun Yang <sup>id</sup>, Sebastian Kram <sup>id</sup>, Maximilian Stahlke <sup>id</sup>, Christopher Mutschler <sup>id</sup>, Sander Coene <sup>id</sup>, Chenglong Li <sup>id</sup>, *Member, IEEE*, Alexander Venus <sup>id</sup>, *Student Member, IEEE*, Erik Leitinger <sup>id</sup>, *Member, IEEE*, Stefan Tertinek <sup>id</sup>, Klaus Witrisal <sup>id</sup>, *Member, IEEE*, Yi Wang <sup>id</sup>, *Senior Member, IEEE*, Shaobo Wang <sup>id</sup>, Beihong Jin <sup>id</sup>, Fusang Zhang <sup>id</sup>, Chang Su <sup>id</sup>, *Graduate Student Member, IEEE*, Zhi Wang <sup>id</sup>, Siheng Li <sup>id</sup>, *Student Member, IEEE*, Xiaodong Li <sup>id</sup>, Shitao Li <sup>id</sup>, Mengguan Pan <sup>id</sup>, *Member, IEEE*, Wang Zheng <sup>id</sup>, Kai Luo <sup>id</sup>, Ziyao Ma <sup>id</sup>, Yanbiao Gao <sup>id</sup>, Jiaxing Chang <sup>id</sup>, Hailong Ren <sup>id</sup>, Wenfang Guo <sup>id</sup>, and Joaquín Torres-Sospedra <sup>id</sup>

**Abstract**—Indoor positioning is a thriving research area, which is slowly gaining market momentum. Its applications are mostly customized, ad hoc installations; ubiquitous applications analogous to Global Navigation Satellite System for outdoors are not available because of the lack of generic platforms, widely accepted standards and interoperability protocols. In this context, the indoor positioning and indoor navigation (IPIN) competition is the only long-term, technically sound initiative to monitor the state of the art of real systems by measuring their performance in a realistic environment. Most competing systems are pedestrian-oriented and based on the use of smartphones, but several competing tracks were set up, enabling comparison of an array of technologies. The two IPIN competitions described here include only off-site tracks. In contrast with on-site tracks where competitors bring their systems on-site—which were impossible to organize during 2021 and 2022—in off-site tracks competitors download prerecorded data from multiple sensors and process them using the EvaAPI, a real-time, web-based emulation interface. As usual with IPIN competitions, tracks were compliant with the EvAAL framework, ensuring consistency of the measurement procedure and reliability of results. The main contribution of this work is to show a compilation of possible indoor positioning scenarios and different indoor positioning solutions to the same problem.

**Index Terms**—Channel impulse response (CIR) positioning, evaluation, fifth-generation (5G) positioning, foot-mounted inertial measurement unit (IMU), indoor navigation, indoor positioning, pedestrian navigation, smartphone-based positioning, vehicle positioning.

## NOMENCLATURE

5G	Fifth-generation technology standard for broadband cellular networks.
AoA	Angle-of-arrival.
AoD	Angle-of-departure.

API	Application programming interface.
BLE	Bluetooth low energy.
CI	Channel information.
CIR	Channel impulse response.
C-SLAM	Channel SLAM.
EKF	Extended Kalman filter.
EMI	Error mitigation.
ENU	East, North, Up.
ESKF	Error-state Kalman filter.
FFT	Fast Fourier transform.
FP	Fingerprinting.

Manuscript received 8 May 2023; revised 25 August 2023, 14 November 2023, and 13 January 2024; accepted 15 January 2024. Date of publication 18 January 2024; date of current version 20 March 2024. (Corresponding authors: Antonino Crivello; Joaquín Torres-Sospedra.)

Please see the Acknowledgment section of this article for the author affiliations and financial support.

Digital Object Identifier 10.1109/JISPIN.2024.3355840

GNSS	Global Navigation Satellite System.
GPS	Global positioning system.
HTTP	Hypertext transfer protocol.
IMU	Inertial measurement unit.
INS	Inertial navigation system.
IPIN	Indoor positioning and indoor navigation.
KF	Kalman filter.
LiDAR	Light detection and ranging.
LLA	Latitude, longitude, altitude.
LLOP	Linear line of position.
LOS	Line-of-sight.
MAE	Mean absolute error.
MCC	Maximum correntropy criterion.
ML	Machine learning.
MU	Moving user.
NHC	Nonholonomic constraint.
NIST	National Institute of Standards and Technology.
NLOS	Non-line-of-sight.
NTP	Network time protocol.
PCA	Principal component analysis.
PDF	Probability density function.
PDR	Pedestrian dead reckoning.
PERSY	Pedestrian reference system.
PF	Particle filter.
pRRU	Pico remote radio unit.
QQ	Quantile–quantile.
RF	Radio frequency.
RSRP	Reference signal received power.
RSS	Received signal strength.
RTOA	Relative time of arrival.
SNR	Signal-to-noise ratio.
SPA	Sum-product algorithm.
SRS	Sounding reference signal.
TAE	Time alignment error.
TOA	Time of arrival.
ToF	Time-of-flight.
TRP	Transmission reception point.
UE	User equipment.
ULISS	Ubiquitous localization with inertial sensors and satellites.
UL-TDOA	Uplink time-difference-of-arrival.
UWB	Ultrawideband.
VO	Visual odometry.
WHIPP	Wica heuristic indoor propagation prediction.
WKNN	Weighted $k$ -nearest neighbours.
ZUPT	Zero-velocity constraint.

## I. INTRODUCTION

THE purpose of the IPIN competition is to create an environment where methods and algorithms for indoor localization can be tested in a controlled environment as realistic as possible [1]. The idea is that localization systems described on papers are next to impossible to compare in a significant way, for a variety of reasons. First of all, the fact that each research group almost always works and tests the system in its own laboratory or *nearby* facility. Second, systems are often complex

and their description may omit some relevant parameters or implementation details, making them impossible to reproduce. Third, but not least important, the infrastructure required to support positioning may not be fully replicated in a different location.

Benchmarking based on public competition is one way out of these problems: research groups are invited to showcase their system in a way that makes it possible to compare it with other systems on an even ground. This article introduces IPIN competition's outcomes for the 2021 and 2022 editions.

The main contributions of this work in relation to previous ones [2], [3], [4], [5] are as follows.

- 1) The introduction of the EvaalAPI, an open source API, that allows off-site tracks to simulate the stressing conditions of an on-site track.
- 2) New tracks added that introduce new challenging scenarios for indoor positioning, such as *Track 8: fifth-generation (5G) in open plan office*.
- 3) New environments and challenges are introduced to already existing tracks.
- 4) Description of state-of-art solutions.

## II. EVAAL FRAMEWORK

The *EvAAL framework* is a set of criteria for defining how an indoor positioning competition should be set up. It was defined in 2014 based on the original EvAAL competitions [6].

During a *competition*, a number of teams compete according to a set of rules, which define a *track*. A competition may include a number of tracks, each centred on different types of devices and each with its own rules. Tracks can be *on-site*, with teams gathering in a physical place to run their working systems, or *off-site*, with no physical gathering and no physical devices involved from the participating team. For each track, competitors run one or more *trials* during which the performance of their systems is measured. In on-site tracks, an *actor* walks along a predefined path while carrying or wearing the competing system, which continuously estimates and records its position along the path. Reference points are marked along the path, and position estimation errors are measured for each reference point.

Competitors have the opportunity to survey the environment, running *testing trials* on their own, before running (usually) two *scoring trials* on which the *competition score* is computed and the final competition ranking is established.

The same applies to off-site tracks, with the main difference being that the competitors do not collect any data, neither for surveying the environment nor for participating in the competition. Data collection tasks are delegated to track chairs. All competitors have the same surveyed data and participate in the competition with the same information.

In short, the EvAAL framework considers the following four *core* criteria:

- 1) natural movement of an actor;
  - 2) realistic environment;
  - 3) realistic measurement resolution;
  - 4) third quartile of point Euclidean error;
- and the following four *extended* criteria:

- 1) secret path;
- 2) independent actor;
- 3) independent logging system;
- 4) identical path and timing.

The criteria are defined and discussed in [6] and analyzed comprehensively in [1].

### A. Integrating Multiple Diverse Tracks

An IPIN competition is in fact composed of several independent competitions, called tracks. Each track has its own rules and purpose. Competitors can participate in one or more tracks. Tracks adhere to the EvAAL framework, though to different degrees. Tracks can be either *on-site* or *off-site* as follows.

- 1) *On-site* tracks are run in real-time, with trials consisting of a real device collecting sensor data and carried by a real person (an *actor*) walking along a predefined path previously unknown to competitors. The device, which runs software written by competitors, continuously estimates and records the current position. Estimates are collected at the end of each trial and handed to track chairs, who then compare them to a ground truth unknown to competitors. In an *on-site* environment, competitors are free to explore the site themselves and make surveys to tune their systems and discover the specifics of the competition area. Usually, this happens the day before the competition proper. During competition proper, scoring is computed on the best of two trials done on the same path.
- 2) *Off-site* tracks are done on recorded data rather than on real-time collected data. Track chairs collect sensor data at a given location and then provide them to competitors. Competitors run their software on the sensor data, estimate positions, and then hand those estimates to track chairs to be compared with the ground truth. In an *off-site* competition, competitors are provided with *training trial data* and/or *testing trial datasets* to check that their system indeed works and tune it as long as they need. Then, they are provided with (usually) two *scoring trial datasets*, on which the scoring is finally computed.

As an example, the flagship track of the IPIN competition has been the on-site Smartphone track, track 1 in the years 2014–2019. The rules of this track have specified that competitors must implement their solution as an app running on a commercial off-the-shelf smartphone, without communicating with the outside world. Only sensors embedded into the smartphone have been allowed, and the use of external devices has been excluded.

### B. Similar Competitions

As it often happens, many people have had the same idea around the same time. In 2011, the first EvAAL competition was held in Valencia (ES) as part of UniversAAL project (FP7-ICT-2009-4), with two more editions in 2012 and 2013.

Microsoft indoor localization competition was also born in 2011, in association with the International Conference on Information Processing in Sensor Networks [7], [8], [9]. The Microsoft competition's aim was to muster different teams around

TABLE I  
BASIC STATISTICS FOR ALL PAST IPIN COMPETITIONS

Edition		On-site		Off-site		Overall	
Year	Location	Tracks	Teams (reg.)	Tracks	Teams (reg.)	Tracks	Teams (reg.)
2014	Busan (KR)	1	7 (11)	—	—	1	7 (11)
2015	Banff (CA)	2	6 (8)	1	4 (4)	3	10 (12)
2016	Alcalá (ES)	2	12 (14)	2	7 (9)	4	19 (23)
2017	Sapporo (JP)	2	10 (18)	2	10 (11)	4	20 (29)
2018	Nantes (FR)	2	15 (17)	2	19 (22)	4	34 (39)
2019	Pisa (IT)	2	10 (16)	3	20 (26)	5	30 (42)
2020	online	—	—	5	22 (32)	5	22 (32)
2021	Lloret de Mar (ES)	—	—	3	13 (26)	3	13 (26)
2022	Beijing (CN)	—	—	6	26 (29)	6	26 (29)

Number of tracks, teams that participated and teams that registered.

the world using as many different approaches as possible, with few constraints. Measurements were taken with the competing systems staying still at a number of reference points, and no attempt at realistic movement or environment was made. The competition was held yearly until 2017.

The PerfLoc Prize Competition was run in 2018 by the NIST (U.S.), while the Positioning Algorithm Competition was run in 2019 by the IEEE Communication Theory Workshop. Both competitions were centred on RF systems [5]. The first responder smart tracking competition is a big and ambitious effort funded (again) by NIST with \$8M, most of which will be awarded to competitors. It was launched in 2022 and is planned to be completed end of 2023.

### C. Previous IPIN Competitions

IPIN competitions started in 2014 in Busan, with a single on-site track based on smartphones. The first off-site track was run in 2015. Years 2020–2022 have not seen on-site tracks because of travel restrictions.

Table I summarizes the location, number of tracks, and number of competitors participating in on-site and off-site tracks during the history of the IPIN competition.

## III. INNOVATION IN 2021 AND 2022 EDITIONS

The lessons learned after organizing the off-site edition of the IPIN Competition 2020 [4] were considered in the 2021 and 2022 editions, which both brought significant innovation as follows:

- 1) the introduction of the EvaalAPI in off-site tracks;
- 2) considering new challenges in existing tracks;
- 3) the birth of several new tracks introducing new localization technologies;
- 4) novel solutions for the different tracks.

### A. EvaalAPI

The EvaalAPI interface is used to run off-site tracks. It was introduced in 2021 as experimental and established in 2022 for downloading testing trials and providing position estimates.

The purpose of the EvaalAPI interface (see Section IV) is to make the results of off-site tracks closer to those of on-site tracks by removing some distortions that became apparent in 2015 when the first off-site track was introduced. Distortions

include, for instance, fixing positions afterward and smoothing scoring trajectory with future information.

### B. New Challenges in Existing Tracks

This is a short summary of new challenges introduced to existing tracks in 2021 and 2022. Each is described in deeper detail in the following sections.

*Track 3:* Smartphone, introduced in 2015, exploits the sensors of a smartphone. In 2015, the competition was based on static Wi-Fi fingerprinting. In 2016, user's motion and other sensors were introduced. In 2018, the first very large scenario was introduced, a shopping mall. In 2021, *device diversity* and *user diversity* were introduced to the track.

*Track 4:* Foot-mounted inertial measurement unit (IMU), introduced in 2018, exploits data gathered by multi-sensor equipment mounted on the foot. The PERSY sensor used in 2018–2020 [3], [4], [5] was replaced by ULISS in 2021 [10], as the latter is able to deliver 3-D inertial and magnetic, pressure, and GNSS data.

*Track 7:* CIR, introduced in 2020, where an actor moves around a warehouse-like environment wearing a tag that regularly transmits UWB signals and CIR readings are gathered by anchors positioned around the area. In 2021, a second scenario without training was provided, where clutter elements from the first scenario were moved within the environment, allowing the assessment of the adaptability to changes in the environment. In 2022, training and evaluation data were collected by different agents and the EvaalAPI was adopted.

### C. New Localization Technologies

This is a short summary of new localization technologies introduced in 2021 and 2022. Each is described in deeper detail in the following sections.

*Camera:* Introduced in 2022, this is the successor to the on-site camera Track 2 run in 2019, but with a different approach. Training data are a set of photographs taken in an apartment, together with the shooting position and orientation; scoring data are more photographs taken in the same environment by a moving actor.

*Vehicle:* Smartphone on vehicle, reintroduced in 2022, exploits sensors of a smartphone attached to a car's dashboard. Training data and scoring data come from a car driving along GNSS-impaired areas and in underground parking.

*5G:* Positioning based on 5G technology standard for broadband cellular networks, introduced in 2022, exploits reference signals sent by 5G smartphones to four base stations installed on the ceiling of an open office. The base stations send measurements

to a location server which estimates the user equipment (UE) location, a method called 5G network-based localization. This track is intended to encourage the development of innovative algorithms for 5G positioning.

### D. Novel Solutions for the Competition Tracks

The indoor positioning community was challenged with several tracks in 2021 and 2022. A total of 26 (2021) and 29 (2022) teams submitted their proposal to participate in the competition, but only 13 (2021) and 26 (2022) submitted their outputs to participate in the competition (see Table I).

The short description of the proposed indoor localization solutions is available on the Evaal website [11]. All teams from the 2021 and 2022 editions were invited to submit an extended detailed description to be reported in this manuscript. Sections V–X include descriptions from those teams that accepted the invitation.

## IV. EVAALAPI

From 2015 to 2020, sensor data recorded by track chairs were timestamped and stored into a file which was then sent to competitors. Competitors would then send back the results some days later, by a common deadline. In time, we observed that competitors were more and more often treating the challenge more like an *optimization* problem than the *emulation* of an on-site trial. Specifically, we observed three main ways where *optimization* differs from *emulation* of on-site behavior, and usually provides more accurate results.

One difference is that on-site trials are *causal*, meaning that estimates provided by competitors are necessarily based only on past sensor readings. This can make a big difference in estimation accuracy, which is important because real localization systems are indeed causal.

Another difference is that on-site trials are *one-shot*, meaning that if something goes wrong in a trial, you can not just retry it. A real localization system cannot ask the user to go back and try again if it detects inconsistencies in its estimation results.

The last notable difference is that on-site trials are run in *real-time*, meaning that estimation is timestamped when it is provided, analogously to a real localization system, which uses the position information as soon as it gets it, in order to provide a smooth experience to users.

The introduction of the EvaalAPI interface in 2021 forced off-site tracks to a behavior, which was causal, one-shot, and real-time behavior, making them more similar to on-site tracks. In the following, the detailed working of EvaalAPI is discussed and some comparisons are made about off-site tracks, which switched to EvaalAPI.

### A. EvaalAPI Concept

To make off-site track behavior more similar to on-site tracks, the first step is to force causal behavior by forcing the competing system to provide position estimates as it reads data from multiple sensors. This is obtained by defining an API for providing sensor data to the competing system and getting position

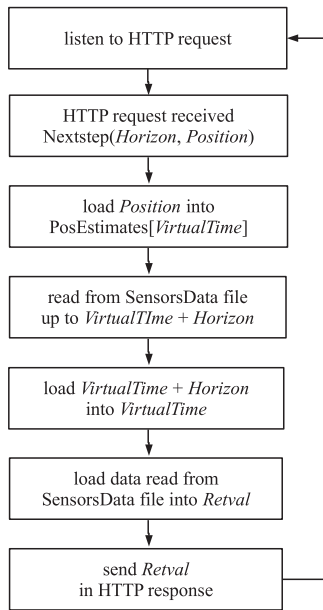


Fig. 1. High-level view of the Nextdata loop.

```

1: procedure TRIAL(SensorsData,PosEstimates)
2:   open SensorsData file for reading
3:   open PosEstimates file for writing
4:   initialise VirtualTime
5:   listen to HTTP Nextdata requests
6:   repeat                                ▷ Wait for HTTP request
7:     Nextdata(Horizon, Position)        ▷ HTTP GE. rcvd
8:     Retval ← []
9:     Deadline ← VirtualTime + Horizon
10:    Position → appendLineTo(PosEstimates)
11:    repeat
12:      DataLine ← nextLineFrom(SensorsData)
13:      Retval[end + 1] ← DataLine
14:      VirtualTime ← DataLine.timestamp
15:    until VirtualTime > Deadline
16:    return Retval                        ▷ Answer HTTP request
17:  until end of SensorsData file
18: end procedure
  
```

Fig. 2. EvaalAPI server data logic.

estimates from it. The API is implemented as a web service. The competing system runs a loop where it repeatedly reads data from multiple sensors and provides a position estimate. The EvaalAPI server reads sensor data from a file, provided by track chairs, where each row is timestamped and contains data from one or more sensors. The server writes position estimates obtained by competitors to a file, which is subsequently used by track chairs to compute the score of the trial.

1) *Forcing Causality—The Nextdata Loop*: The EvaalAPI server waits for a Nextdata (*Horizon*, *Position*) command [an HTTP request] from the competing system acting as a client; it answers the request with timestamped sensor data, which it reads from the data file. Figs. 1 and 2 illustrate the server loop. In each iteration of the main loop, the client sends a Nextdata command. Each carries a position estimate, which the client has computed on the sensor data received from previous Nextdata commands, and a requested time horizon, indicating how much sensor data the client expects as an answer to the request.

TABLE II  
BEST SCORES IN METres (FIRST AND SECOND PLACE) FOR ON-SITE AND OFF-SITE SMARTPHONE TRACK BEFORE AND AFTER EVAALAPI WAS INTRODUCED IN 2021

Year	T1: on-site		T3: off-site	
	winner	second	winner	second
2014	5.7	6.6	—	—
2015	6.6	10.0	8.3	10.9
2016	5.4	8.2	5.8	7.3
2017	8.8	16.8	3.5	3.5
2018	—	—	0.9	1.3
2019	3.8	7.4	2.3	2.4
2020	—	—	1.0	1.7
2021	—	—	4.4	7.9
2022	—	—	30.1	39.8

This interface forces *causal behavior* because the competing system can base its position estimates only on past (in virtual time) sensor data; it can exploit no forward knowledge.

2) *Forcing One-Shot—Nonreloadable Trials*: In order to force *one-shot behavior*, each *scoring trial* can be run only once, i.e., it is *nonreloadable*. Each Track provides a number of *testing trials*, i.e., *reloadable* ones, that can be used at will by competitors to tune their system. In addition, it provides a few (usually two) *scoring trials*, which can be run only once, on which the score is computed, and the best one used for ranking the competitors.

3) *Forcing Real-Time—Managing Timeout*: In order to force *real-time behavior*, the virtual time is linked to the wall time. Virtual time is relative to the time stamped on each line of the sensor data file and to the *horizon* used in each Nextdata (*Horizon*, *Position*) request.

EvaalAPI forces real-time behavior by slowing down virtual time with respect to wall time by a *slowdown factor*  $V$  ( $V \geq 1$ ), to account for network delays, transmission bottlenecks and server response time. In practice, EvaalAPI implements a leaky bucket with a rate defined by the slowdown factor and a threshold useful for compensating occasional brief networking disruptions; a timeout occurs when the bucket empties.

## B. EvaalAPI Implementation

Source code, including a demo program written in Python, is available and licensed under a GNU Affero General Public License [12], which allows anyone to use, modify and redistribute it freely.

## C. EvaalAPI Experience

Results from the competition have shown that EvaalAPI has made a difference. This is most clear when looking at results from tracks 1 and 3, given in Table II, which summarizes the best scores. Tracks 1 and 3 are the oldest and more stable ones. They are based on the same technology and are run in similar environments, that is, using sensors from a smartphone in big office environments. Notably, in 2019 tracks 1 and 3 shared the same location and even some of the reference points.

During the five on-site smartphone competitions, winning teams have always obtained scores in the range from approximately 4 to 9 m, which is the same that happened in the first

three years of the off-site competition. In 2018, scores from the off-site track started to diverge, becoming much better than those of the on-site one. This was even more clear in 2019, when the preparation phase—choosing the path and taking measurements—was done by the same people in the same area for both the off-site and the on-site tracks.

In 2021, with EvaalAPI, the off-site track results were back again to realistic numbers. In 2022, results were bad, apparently because the competition was more difficult with respect to 2021. In 2023, tracks 1 and 3 shared the same environment and the same sensors: results, yet to be published, show again a realistic alignment between them.

## V. TRACK 2: CAMERA (2022)

This section describes track 2, which was based on camera (computer vision) and took place only in 2022.

### A. Track Description

The widespread availability and the combination of sensing, computation, and communication capabilities make smartphones an attractive platform for indoor localization. The preferred localization approaches are influenced by factors, such as infrastructure availability, size, and type of the target indoor site, people’s movement characteristics, desired frequency, latency, and accuracy of the localization result.

Image-based localization does not require the presence of specific infrastructure, can handle relatively large sites, and can provide orientation along with position estimation. Although it is possible to obtain centimeter-level accuracy for room or apartment-sized sites, in practical applications, achieving and maintaining similar accuracy in large public areas remains challenging. Among the relevant issues contributing to this challenge are variability in visual appearance over time, irregular motion patterns and the presence of dynamic objects.

The aim of the track 2 competition is to test image-based indoor localization for pedestrians. The target site was two floors of an office building with a test area of about  $50\text{ m} \times 50\text{ m}$  per floor. Using a smartphone, we collected image and sensor data but focused on using only image data for localization mainly due to the off-site setting of track 2.

The training data limited site coverage to simulate requirements for simplified collection procedures. The scoring trials’ data featured reduced frame rate and larger motion variability including stopping, sitting/standing and meandering. The reduced frame rate was partially motivated by a general preference for solutions with lower power consumption and partially by practical time constraints for scoring trials in settings with limited internet connection speed.

### B. Environment and Measurement Setup

Track 2 used three floors of an office building. Data from the third floor (site 1) were used for training and were provided to competitors in advance. Data from the other two floors (site 2) were collected along the trajectories shown in Fig. 3 and divided into training (plotted in green) and testing (plotted in yellow and

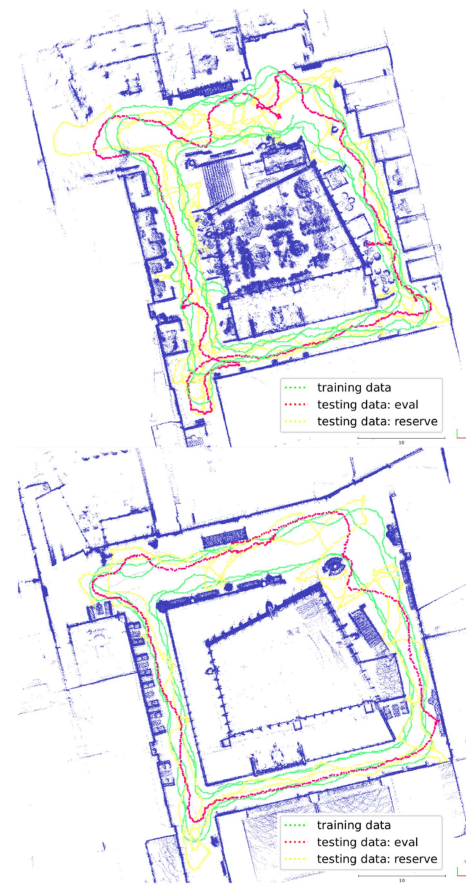


Fig. 3. Data collected at track 2 evaluation site 2—floor 1 (top) and floor 2 (bottom). From the collected testing data trajectories, two (red) were used for scoring trials and the rest (yellow) were kept in reserve.

red) sets. The training data were provided to the competitors on the day before the scoring trials. Two trajectories from the testing data (red trajectories) were used for the scoring trials on the competition day.

To obtain ground truth labels, a backpack setup with a LiDAR (HESAI Pandar-QT) was used to scan the site and build a localization map. Later, images ( $640 \times 480$ , 30 fps) and sensor data were collected using a smartphone (SM-N986 N). Training data were collected sequentially by several subjects walking along the hallway in a closed loop, holding the smartphone in their right hand in front of the body, with the rear camera facing forward. The recorded pose (longitude, latitude, floor, orientation) was the pose of the subject and a reasonable effort was made to keep a steady offset of the smartphone relative to the body.

For training data, 43 524 images were recorded along four closed trajectories per floor, combining the inner and outer sides of the hallway with clockwise and counterclockwise directions. For testing data, 5244 images were recorded along seven closed trajectories, keeping each trajectory on a single floor. Unlike the training data, the testing data trajectories included larger variations in walking speed (with stopping and sitting) and direction. Two test data trajectories were selected for scoring trials on the competition day. The image frame rate was reduced

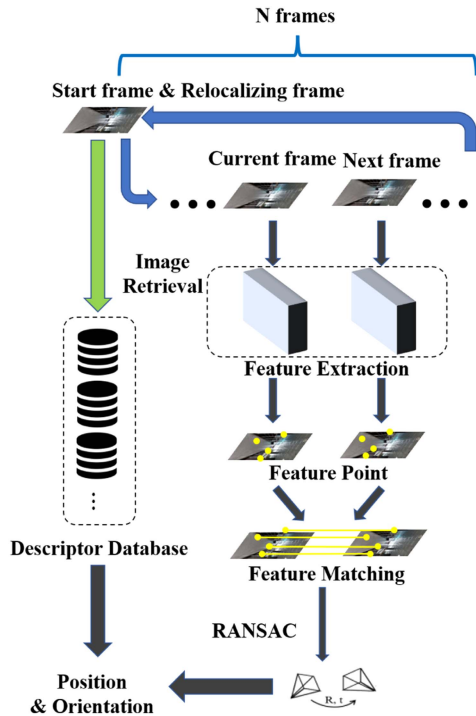


Fig. 4. Team CamLoc system architecture.

to 3 fps and reference points were selected for error evaluation. Scoring trial 1 had a length of 170 m, with 735 images and 80 reference points. Scoring trial 2 had a length of 136 m, with 750 images and 64 reference points.

### C. Description of Competitors (Camera)

1) *Team CamLoc*: In this competition, the team realized a visual localizing system based on an image retrieval algorithm and VO. The system architecture can be seen in Fig. 4. The overall process of the whole system can be divided into the following parts.

a) *Step 1 Build image descriptor database*: To localize the smartphone with an image retrieval algorithm, an image descriptor database needs to be built in advance. Patch-NetVLAD [13] model was used to extract the descriptor vector for each image in the training dataset and save them as files for the following image retrieval step.

b) *Step 2 Image retrieval*: During the test, the Patch-NetVLAD model was used to extract the descriptor of the query image online. The similarity between the query image and images in the database will be calculated. The approach finds the most similar image in the database and uses its ground truth as the pose of the query image. In order to speed up the process of similarity calculation, keyframes from the image descriptor database for every 20 images are selected. Since image retrieval is a type of nonincremental localizing algorithm, it is used to predict the starting point and relocalize, which can reduce the cumulative error from the following VO step.

c) *Step 3 VO*: It is time-consuming and less generalizable for each test image to retrieve a similar image in the database. So, a frame-by-frame monocular VO is implemented to locate the smartphone in a faster and more robust way, which enables the system to track the smartphone even in an unknown environment. For the sake of getting high-quality feature points and their matching relationship, SuperPoint [14] and Super-Glue [15] models were used in Team CamLoc’s system. To make the monocular VO work effectively, the team needs to align the pose and estimate the scale factor. The poses predicted by VO are in the camera coordinate system, so the pose between the VO coordinate system and the LLA coordinate system were transformed with the help of the ENU coordinate system. Since VO is a type of incremental localizing algorithm, the problem of cumulative error is inevitable. To solve the problem, the system relocalizes with image retrieval for every  $N$  frames. In practice,  $N$  is set to 30. As for the scale factor, the prediction and ground truth on the training dataset were aligned with the Umeyama algorithm to get the estimated scale parameter.

## VI. TRACK 3: SMARTPHONE (2021 AND 2022)

This section describes track 3, which was based on the use of smartphones and took place in 2021 and 2022.

### A. Track Description

The objective of track 3 is to evaluate the performance of different integrated navigation solutions based on regular smartphone sensor fusion (WiFi, Bluetooth, and inertial, among others) in an *off-site* context. As done in the 2016–2020 editions [2], [3], [4], [5], [16], a data collection strategy and evaluation procedure has been followed.

All data for track 3 has been collected with the Android app “GetSensorData” [17], [18], which records and stores all data coming from sensors available in the smartphone into a single text file, i.e., into a *logfile*. As usual, the dataset is split into three independent subsets, namely, training, validation, and evaluation using ML terminology. A novelty introduced in 2021 was the evaluation through the EvaalAPI, renaming those subsets into training trials, testing trials and scoring trials, respectively.

The first set is for calibration purposes and covers most of the evaluation area, containing several simple short single-floor tracks with several key points at relevant positions including initial, final and turns in the tracks. In the training trials, the trajectory between two key points is almost straight.

The second set is for validation. It contains useful data for competitors to evaluate their systems with long trials covering multiple floors and well-known locations for the key points. Generally, testing trials only include a few key points and the user’s movement is not restricted to straight lines between two consecutive key points. In addition, new areas might be explored. Testing trials allow the competitors to evaluate the accuracy of their solutions as many times as they wish, getting an assessment of the level of maturity of their solution.

The third and last set is devoted to evaluation purposes, allowing competitors to have an independent external evaluation without ground truth data, and contains three multifloor very

**TABLE III**  
SMARTPHONES USED IN TRACK 3 (2021 AND 2022) DETAILING THE COMMERCIAL NAME, THE MANUFACTURER CODE (IF ANY), THE ANDROID VERSION, THE SENSORS USED, AND THE EDITION WHEN THE SMARTPHONE WAS USED

Commercial name	Codename	Ver.	Acce/Gyro	Magn.	Pres.	Edition
BQ Aquaris X5 Plus	–	7.1.1	BMI160	AK09916	N/A	2022
Google Nexus 5	–	6.0.1	MPU6515	AK8963	BMP280	2022
Samsung Note 9	SM-N960F	10	LSM6DSL	AK09918C	LPS22H	2021/22
Samsung Note 10	SM-N975F	11	LSM6DSO	AK09918C	LPS22H	2021
Samsung A31 5G	SM-A315G	11	LSM6DSL	YAS539	N/A	2022
Samsung A52	SM-A528B	12	LSM6DSO	AK0991X	N/A	2022
Samsung A5 2017	SM-A520F	8.0.0	K6DS3TR	AK09916	LPS25H	2021/22
Samsung S7	SM-G930F	8.0.0	K6DS3TR	YAS537	LPS25H	2021/22
Xiaomi Mi 10 Pro	–	10	LSM6DSO	AK0991X	BMP285	2021
Xiaomi POCO X3	M2102J20SG	11	LSM6DSO	AK0991X	N/A	2022

long tracks. In contrast to the systematic data collection done in the previous trials, the scoring trials include realistic movements (e.g., simulating a user that was messaging or taking a phone call) and stops. Only three unlabelled scoring trials were provided to competitors in each edition. The accuracy score of a scoring trial corresponds to the 75th percentile of the *sample error* in compliance with the Evaal framework. This error is the 2-D positioning error plus a penalty of 15 m times the absolute difference between the current and the estimated floors. The team's score corresponds to the best (lowest) score among the three scoring trials.

The main difference introduced in 2021 with respect to the previous editions was the incorporation of several devices and users instead of collecting all data with the same device, i.e., track 3 chairs challenged the competitors with device diversity. In 2021, training and validation data were collected with five smartphones, which are detailed in Table III. The table illustrates the range of sensors considered in the competition. For evaluation in 2021, two scoring trials collected with a Samsung S7 by two different users and a scoring trial collected with a Samsung A5 2017 were provided.

This *device diversity* feature was kept in 2022 but with a different and larger subset of phones, as shown in Table III, only a few phones were used in both editions. For evaluation in 2022, three scoring trials were provided, collected with the smartphones BQ Aquaris X5 Plus, Samsung A31 5G, and Samsung A5 2017, respectively.

Given the large amount of data and diversity of smartphones, a reasonable sampling frequency was set in “GetSensorData” for all sensors to record at 100 Hz in both editions, 2021 and 2022.

In addition to the logfiles, georeferenced floor plans are provided to competitors. Those floor plans may be useful at the sensor fusion level, allowing competitors to check whether the provided positions are coherent with the environment.

The logfiles, supplementary materials and full technical descriptions are available in [19] and [20]. This package complements the ones from the previous editions [21], [22], [23], [24], [25].

## B. Environment and Measurement Setup (2021)

For the 2021 edition, competition data came from the facilities of the University of Extremadura (Badajoz, ES). The collection lasted four days and was restricted to the external car park area,

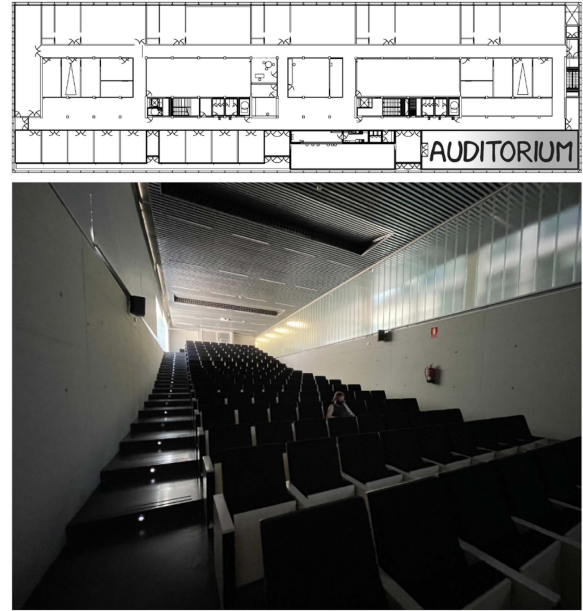


Fig. 5. Floor plan of track 3 (2021) environment and its auditorium (located on the bottom-right corner in floor 1).

the ground floor and the basement. More than 30 BLE beacons were deployed in part of the environment to support indoor positioning, and their location was provided to competitors.

The indoor area included an auditorium, which covers a large area with a soft floor transition as shown in Fig. 5.

## C. Environment and Measurement Setup (2022)

In 2022, competition data came from the facilities of the University of Minho (Guimarães, PT). The collection lasted four days and was restricted to the School of Engineering, a three-storey building, and its surroundings. This time, no additional infrastructure was deployed to support indoor positioning. In addition, the scoring trials were collected one month after the training and testing trials.

The indoor area is a three-storey variable-height building and it includes a large open patio as shown in Fig. 6.

## D. Description of Competitors (Smartphone)

1) *Team Leviathan*: The proposed system consists of the following four components.

- 1) PDR system based on step detection and stride length estimation.
- 2) ESKF incorporating IMU measurements, headings and PDR output.
- 3) Floor detection and initialization based on Wi-Fi fingerprint and barometer.
- 4) PF that utilizes the floor plan information.

The flow chart of the proposed system is shown in Fig. 7.

a) *Pedestrian Dead Reckoning*: The PDR algorithm estimates the pedestrian step count, stride length and heading. Thus, PDR exploits accelerometer, gyroscope, and magnetometer data. To remove high-frequency noise, a low-pass filter is



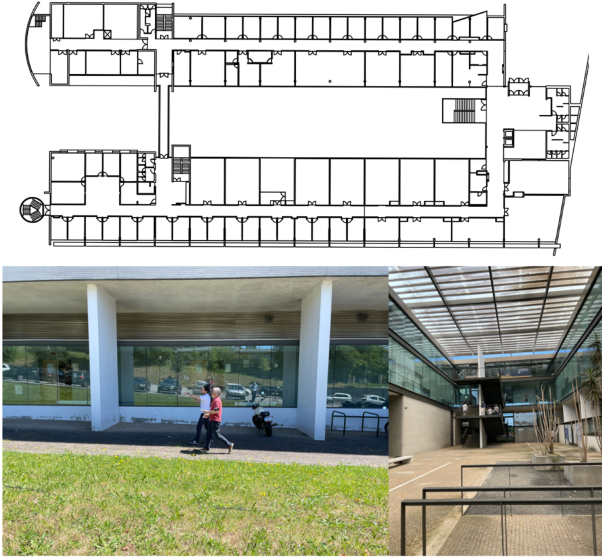


Fig. 6. Floor plan of track 3 (2022) environment and its patio.

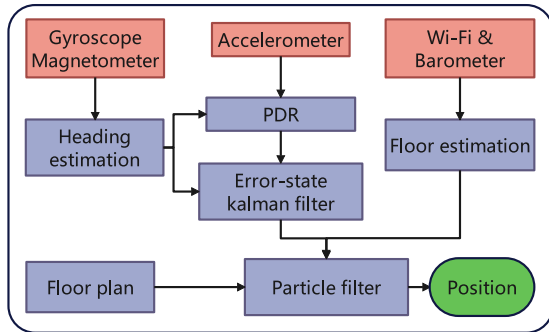


Fig. 7. Flow chart of the indoor localization solution proposed by team Leviathan.

applied to the norm of the acceleration. Team Leviathan first employ FFT to convert acceleration data from the time domain into the frequency domain to better represent the periodic component in the signal [26]. Then, detection is used to identify the steps. Unlike traditional stride length estimation, Leviathan’s approach is more adaptive in the sense that it is formulated as a function of the peak frequency [27]. The heading of the pedestrian is initialized and updated by using the Madgwick method, which combines magnetic field and angular velocity [28].

**b) Error-State Kalman Filter:** In the scenario of indoor localization, the types of sensors used may be different. An EKF is well-known to fuse different kinds of observations together. Compared with EKF, ESKF applies optimization based on the error state, which is numerically small. Thus, the estimation error is smaller during the linearization process, leading to a more accurate result. In the prediction step, the gyroscope and acceleration are used to estimate the current pose. The magnetometer and the PDR result are used to correct the pose estimation. Specifically, the PDR module measures the displacement, and the magnetometer measures the current heading. The observation error is assumed to follow a Gaussian noise distribution to correct the pose estimation.

**c) Floor Detection and Initial Position and Pose Estimation:** The Wi-Fi RSS fingerprint and the barometer are used for floor detection, initial position estimation, and position correction. RSS is susceptible to various environmental changes, e.g., concrete walls, moving humans, temperature and humidity [29]. Compared with PDR, Wi-Fi localization is less accurate. Thus, Wi-Fi RSS is mainly used for position correction and floor detection. A radio map is built from the training data, and the first few Wi-Fi detections are used to locate the initial pose. The variance of the barometer is used to detect the floor change by setting a threshold. The current pose is continuously matched with Wi-Fi location and floor information. Once a significant mismatch is detected, the system resets. Data from the accelerometer and the magnetometer are used to extend positions to pose estimations by adopting the Madgwick filter.

**d) Particle Filter:** The PF fuses the trajectory estimated by the ESKF and compares it with the floor plan to regulate the distribution of particles. The floor plan images are first stored as an obstacle probability map. The floor estimation component first identifies the floor ID and an initial position guess. Each point  $\mathbf{x}$  on a 2-D plane can be assigned with a Gaussian probability distribution

$$\mathcal{L}(\mathbf{x}) = \frac{1}{\sigma\sqrt{2\pi}} \exp\left(-\frac{\min_{\mathbf{x}^* \in \Omega_{\text{obs}}} d(\mathbf{x}, \mathbf{x}^*)}{2\sigma^2}\right) \quad (1)$$

where  $\Omega_{\text{obs}}$  is the set of obstacles,  $\mathbf{x}^*$  is the location of the nearest obstacles, and  $d(\bullet)$  is the Euclidean distance between two points. During each update, a single particle infers its position and the associated probability of hitting an obstacle. In the resampling stage, particles in unreachable areas are removed. Moreover, to account for history information, a particle will be removed if its accumulated penalty within the time window exceeds a predefined threshold. New particles are generated following the distribution of valid particles. The final position is calculated as the weighted average of the particle positions. In case of system failure, i.e., when all particles hit obstacles or a wrong floor ID is reported by the floor detector, random particles will be generated on the specific floor until system convergence.

**2) Team imec-WAVES 2021 and 2022:** Team imec-WAVES’ systems for the 2021 and 2022 competitions are similar and consist of six modules. Each module has the same functionality in both versions, but some modules are implemented differently. Fig. 8 shows how these six modules and their components interact. The following paragraphs briefly describe each module. The description applies to both years unless specified otherwise.

**a) EvalAPI interface:** This interface starts the EvalAPI trial and requests the next stream of smartphone data in blocks of 0.5 s. It parses and structures the received data and passes it to the PDR module, which employs a step detection algorithm (see Section VI-D2b). If the PDR module detects one or more steps, the interface waits for the path estimation algorithm to provide a new position. If no step is detected, the interface will take the previous position estimation. The position is sent back to the EvalAPI server, and a new block of data is received.

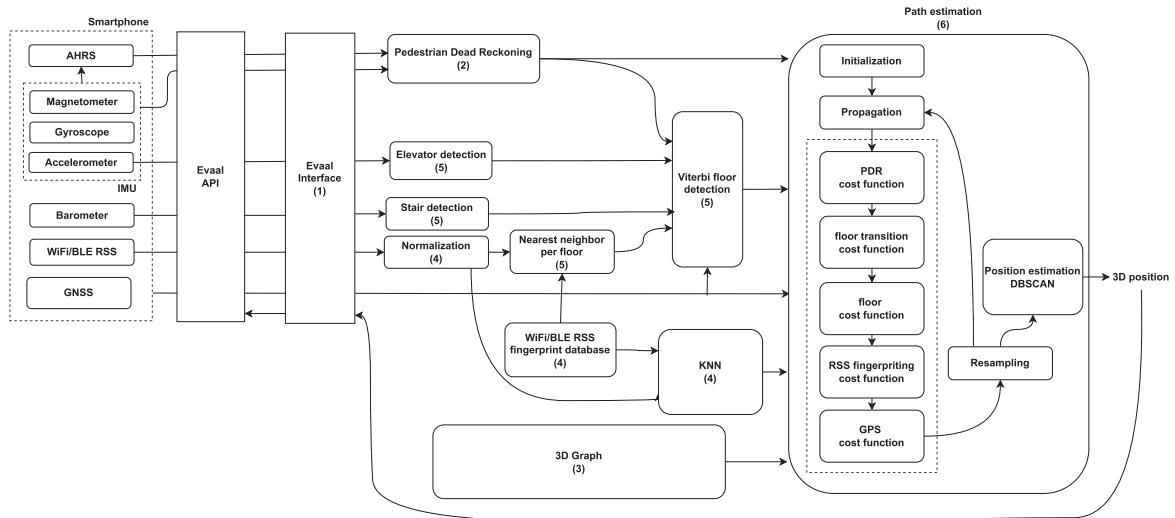


Fig. 8. Flow graph of the systems of team imec-WAVES for track 3 in 2021 and 2022.

*b) Pedestrian Dead Reckoning:* The proposed PDR algorithm is based on [30]. It uses attitude and heading reference system (AHRS), that is, pitch and roll data to transform the accelerometer, gyroscope and magnetometer data from the local (smartphone) reference frame to the horizontal plane. Step detection is performed by detecting peaks in vertical acceleration. The heading is estimated by fusing the horizontal gyroscope and magnetometer data. The adaptive step length estimation is based on the Weinberg model and reproduced from [31]. The fusion algorithm works best when the gyroscope and magnetometer headings are initially aligned. The alignment, as well as gyroscope calibration, is done near the start when the smartphone is held still for several seconds. This time interval is detected by thresholding the acceleration variance.

*c) Graph database of the environment:* Each year, floor plan images of the building are provided. Team imec-WAVES manually draw the walls over the floor plan using the graphical interface of the WHIPP tool [32]—resulting in a line segment for each wall—and also draw over the contours of elevator shafts and staircases, resulting in a polygon for each staircase or elevator shaft. For outdoor trajectories, Google Earth was used to draw the boundaries of the pavement directly surrounding the building. The line segments and polygons are used directly by the path estimation algorithm in the 2021 system.

However, calculating intersections and solving the point-in-polygon problem ad hoc is time-consuming and limits the number of usable particles under EvaalAPI’s timeout constraint. Therefore, a 3-D graph was generated from the set of line segments of each floor in 2022. Each graph node is a possible location. Two nodes are connected by an edge if the latter does not intersect a wall and its length is shorter than a specified maximum human step length. Using the contours, each node knows whether it is a stair, elevator, or floor node and whether it is an indoor or outdoor node. The height of each floor is estimated by converting the pressure data [33] from the training log files, and a 3-D graph is then created. Finally, the floors are connected by drawing the staircases with a custom tool. Result is in Fig. 9.

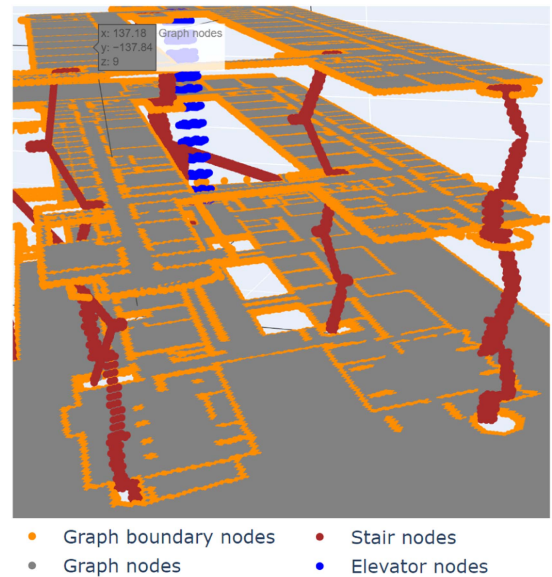


Fig. 9. 3-D graph of the environment of track 3 in 2022.

*d) RSS fingerprinting:* The training data include ground truth positions at turning points. In 2021, the team used a PDR-based method to construct RSS radio maps, known from the previous competition [3]. Since this method does not work well for staircases, the Dijkstra algorithm is used with the 3-D graph in 2022 to create a path on the staircase and match this path with the PDR output.

Furthermore, several BLE beacon locations were provided in 2021. Therefore, RSS prediction [32] is used to create radio maps, which cover most of the building, in addition to the empirical radio maps covering only the training trajectories.

A WKNN fingerprint matching algorithm is used to estimate the user position. The Euclidean distance metric is used to match RSS vectors in the validation/evaluation data with RSS vectors in the radio map. RSS normalization is used to avoid device

mismatch [34]. The weighted centroid of the  $k$  best matches is selected as the estimated position.

*e) Floor (transition) detection:* Floor levels and transitions are detected by fusing data from the pressure sensor, accelerometer, and RSS fingerprinting into the Viterbi-based algorithm described in [35]. In both years, there was an outdoor environment consisting of two levels. Therefore, the team regards these outdoor levels as separate floors, and expands the team's existing algorithm with a simple GNSS-based outdoor detector. If the GNSS coordinate lies outside of the building, a large cost to all indoor states and vice versa was added.

*f) Path estimation:* After each step detection, a new 3-D position is estimated by fusing information from PDR, floor (transition) detection, RSS fingerprinting, and a 3-D graph of the environment (2022) or floor plan information directly (2021). Path estimation in 2021 was performed by a PF, described in detail in [36]. It includes a reset mechanism that removes almost all particles when the PF gets stuck. New particles are sampled randomly in the neighbourhood of the previous sample mean. Also, if there are no particles on the currently estimated floor (including outdoor levels), and the floor has not changed during the last five steps, all particles are randomly resampled on that floor. The same applies to stair detections.

A new path estimation was used in 2022, which combines the PF from 2021, and Viterbi-based tracking from [37]. After step detection, each of the  $N$  particles has to search all the  $K$  reachable nodes and spawn a particle at each node. These  $N \times K$  new particles inherit the cost of their predecessors and receive a new cost based on how well the length and angle of the edge between the new and previous node match. There are additional costs based on RSS fingerprinting, floor detection, and floor transition detection for indoor, similar to PF in [36]. The particles are then resampled based on their cost, and the latest position is estimated by a clustering algorithm based on [36], in which the particle with the lowest cost is the first particle of the cluster. Lastly, if the estimated floor is outdoors, each particle is also evaluated based on its Euclidean distance to available GNSS coordinates in both systems.

*3) Team X-LAB:* The system proposed by X-lab includes the following three main stages:

- 1) the 2-D position estimation based on PDR algorithm;
- 2) the Wi-Fi, Bluetooth, geomagnetic information fusion, and 2-D position correction;
- 3) the initial position estimation and floor decision making.

Six types of sensor data were used in the whole processing of pedestrian positioning. Fig. 10 shows the framework of the proposed system. In the following paragraphs, each stage is explained in detail below.

*a) PDR:* The PDR algorithm consists of step detection, step length estimation, heading estimation, and movement modes recognition. Peak detection is used to detect steps, and the Weinberg method is used to estimate step length. The heading of pedestrians is calculated by gyroscope data. The heading is corrected by a KF algorithm using geomagnetic data to solve the error accumulation problem. In Team X-Lab's system, a support vector machine is used to identify four movement modes, including normal walking, walking upstairs, walking downstairs, and

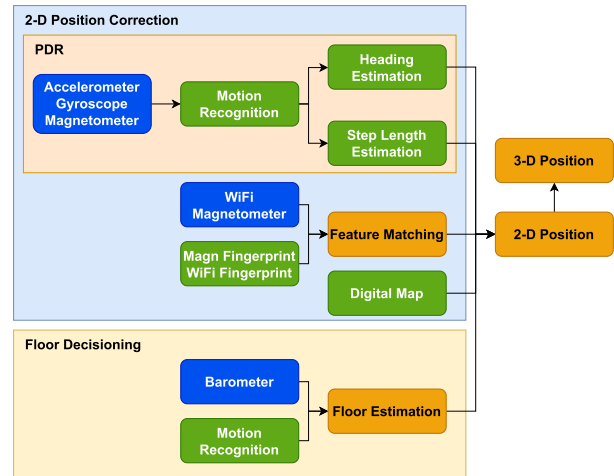


Fig. 10. Framework of the proposed system.

other movements. Some statistical characteristics (e.g., mean, max, min, and derivative) of the accelerometer and gyroscope are extracted as features. The result of the movement modes recognition will influence the selection of parameters in the other three stages.

*b) Information fusion and 2-D position correction:* There are two phases in this stage. The feature map construction in the preparation phase and 2-D position correction in the real-time positioning phase.

In the preparation phase, the Wi-Fi fingerprint, bluetooth fingerprint, and geomagnetic fingerprint map were built. Only a small amount of reference position information is provided in the training data. Therefore, it is necessary to calculate the pedestrian position between two reference position points to obtain more fingerprint information by the PDR algorithm in the previous stage. To improve the accuracy of fingerprint localization and the efficiency of the localization algorithm, PCA is used to eliminate fingerprint information that is not helpful for localization.

In the real-time positioning phase, particle filtering is used to correct the pedestrian position. First, the particles are initialized and the position of the PDR estimate is sampled. Then, the weights of each particle are calculated by feature maps and digital maps. Finally, the resampling process is used to obtain the corrected pedestrian positions. The digital map was created from a map of the buildings provided by the organizers. It contains passable and impassable areas.

*c) Initial position estimation and floor decision making:* The initial position is provided by fingerprint information matching, specifically Wi-Fi, bluetooth, and geomagnetic information matching. The barometer data are used to calculate the relative height, and the result of movement modes recognition is used to judge the floor jointly.

## VII. TRACK 4: FOOT-MOUNTED IMU

This section describes track 4, which was based on the use of foot-mounted IMU and took place in 2021 and 2022.

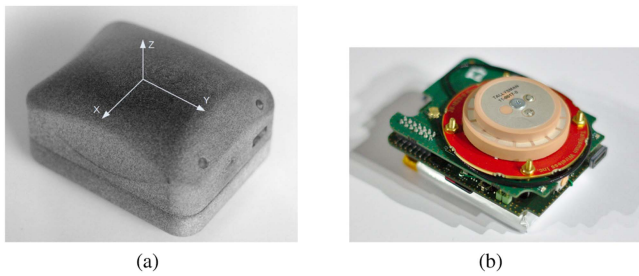


Fig. 11. ULISS overview. (a) External package. (b) Internal overview.

### A. Track Description

The objective of track 4 is to estimate the position from data gathered by multisensor equipment mounted on the foot of an actor walking a predefined path. Since track 4 is focused on the real use cases of pedestrian navigation, *scale* and *scenario* were considered.

Scale stands for the size of the experimentation area: we organized IPIN competitions in a large shopping mall around Nantes in 2021 and in the train station of the same town in 2022. This allowed us to realize trials longer than 30 min and longer than 1 km over areas several hundreds of meters wide and long.

Track 4 gives importance to the quality of representativeness of a scenario. This means that we design our data collection scenario by thinking about the real movement of a specific citizen in a specific place: this year, a tourist visiting an automotive museum. An example to illustrate: navigating through a crowd inside a wide area is something pretty common for citizens, and even if this is not the easiest context for positioning system and algorithm, it deserves to be tackled.

The target environments exhibited features, such as multifloor levels, stairs, escalators, and lifts, everything that is commonly used in public places. This is a perfect mix of a citizen's day-life scenario and scientific challenges for high-level competition.



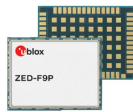
Sensors' data were gathered through the ULISS sensor device [10], which is able to deliver 3-D inertial data (accelerometer, gyroscope), 3-D magnetic data, pressure data and GNSS data. Fig. 11(a) and (b) shows, respectively, an overview of ULISS and its embedded sensors. Table IV presents the technical specifications of all the sensors embedded in the ULISS. More detail can be found in the 2021 call for competition [38].

In compliance with the Evaal framework, in track 4, the accuracy score is computed as the 75th percentile of the *sample error*. As in track 3, the sampling error is itself defined as the sum of 2-D horizontal error plus 15 m per floor misdetection (absolute difference between current floor and estimated floor). The 2-D horizontal error is the Euclidean distance between the estimated horizontal position computed by the competitor and the ground truth position of reference points (85 points in 2021 and 90 in 2022).

### B. Environment and Measurement Setup 2021

In 2021, the competition trajectory was inside the Atlantis shopping mall in Nantes (one of the biggest in the west of France).

TABLE IV  
TECHNICAL SPECIFICATIONS OF THE EMBEDDED ULISS SENSORS

Sensors	Short description
	Xsens Mti-7: <ul style="list-style-type: none"> <li>• 3-D accelerometer: +/- 16 g</li> <li>• 3-D gyroscope: +/- 2000°/s</li> <li>• 3-D magnetometer: 8 G</li> </ul>
	Bosch BMP280: <ul style="list-style-type: none"> <li>• Pressure: 300...1100 hPa</li> </ul>
	Ublox F9P: <ul style="list-style-type: none"> <li>• Multi constellations</li> <li>• Dual GNSS Bands</li> <li>• Raw data under RINEX 3.04 format</li> </ul>

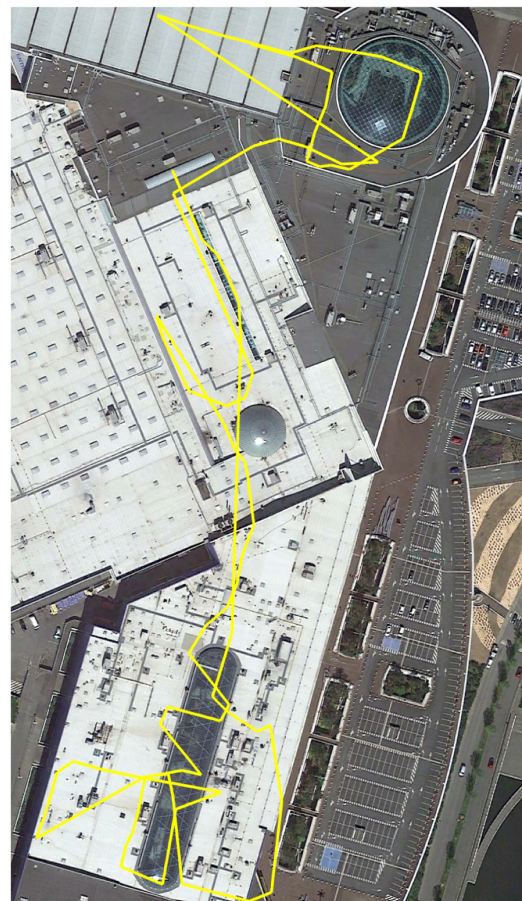


Fig. 12. Overview of the ground truth of track 4 (2021).

Each of the two scoring trials is a trajectory of 45 min duration, about 1.2 km long, where almost 95% of paths are indoor. Active walking (including running) and passive motion (usage of lifts, escalators, and travelators) were used over four different floors. Fig. 12 illustrates a bird's view of each point composing the ground truth.

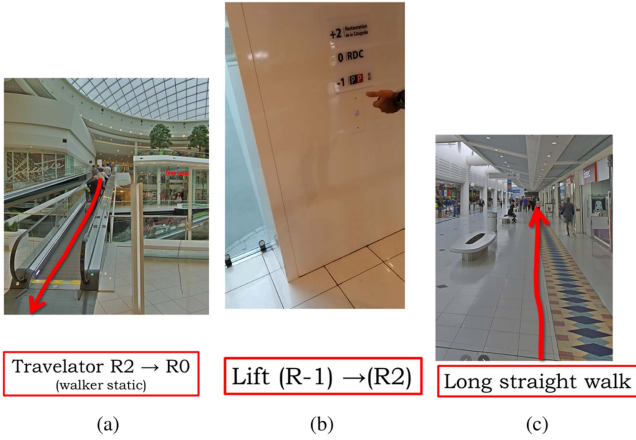


Fig. 13. Some areas where track 4 took place (2021). (a) Travelator. (b) Lift. (c) Straight walk.

Some of the different areas of Atlantis shopping mall used are illustrated in Fig. 13. See the 2021 awards presentation at [39] for additional details.

C. Environment and Measurement Setup 2022

In 2022, the competition data was collected on 12th July in the railway station of Nantes.

A full-body wearable device developed by Xsens called AWINDA was used to provide ground truth. Originally designed for motion capture, it was able to generate a satisfactory ground truth after intensive post-processing. The advantage of using Awinda for ground truth is that we can get ground truth without having to walk on predefined waypoints on the ground as in previous years. The main disadvantage is that both systems (ground truth and competition sensors) need to work perfectly at the same time. Any problem or bug in either system means a new data collection that needs to be done.

Each of the two scoring trials includes a walk of about 1.5 km long in 25 min. Approximately 95% of the walk was done indoors. Only active walking over four different floors without elevators or escalators was used. This is one of the limitations introduced with the new ground truth system. Fig. 14 illustrates a bird’s eye view of the ground truth for the first scoring trial. Some of the different places<sup>1</sup> of Nantes railway station is shown in Fig. 15

Additional detail can be found in the Call for Competition relative to track 4 [40], and the awards presentation [41].

D. Description of Competitors (Foot-Mounted IMU)

1) Team X-lab: The solution presented by X-lab consists of three steps plus a correction model.

a) Step 1: The IPIN2022 competition evaluates the algorithm in real-time, so it is unknown which mode the tester is travelling in and the threshold for zero-velocity detector varies from different modes. There is no way a perfect threshold can be

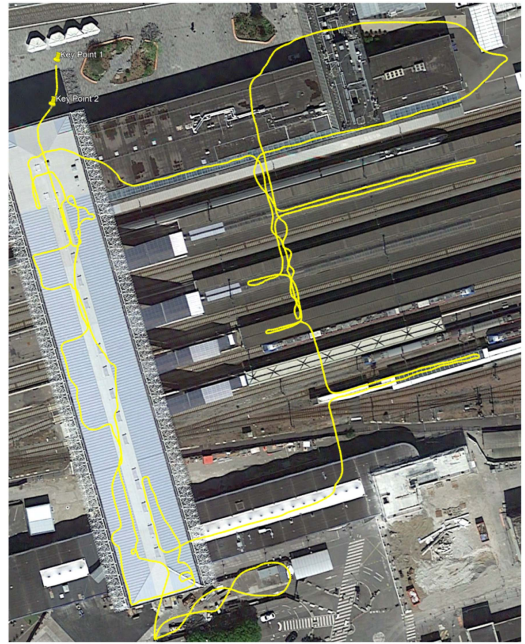


Fig. 14. Overview the ground truth of track 4 (2022).

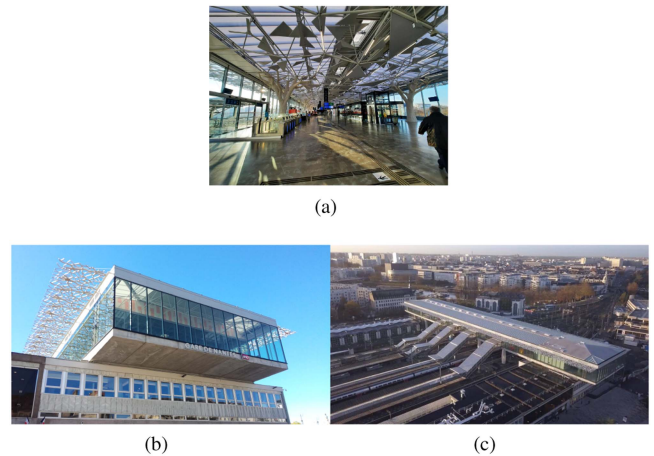


Fig. 15. Views of Nantes railway station. (a) Second floor. (b) Main entrance. (c) Drone view.

set in the algorithm to perfectly exploit the advantages of ZUPT. In this case, the first step is to propose an adaptive zero-velocity detector that is dependent on the tester’s motion modes. The team’s algorithm is based on the fact that the more violent the tester’s motion, the larger the threshold of the zero-velocity detector should be to detect a shorter still phase as possible, while also noting that missed detections are more easily forgiven than false detections, hence the used adaptive zero velocity detector has a relatively small threshold.

b) Step 2: Considering that the biggest shortcoming of ZUPT is the severe heading drift and the lack of reliable heading observation, the heading drift can be corrected to some extent by correcting the pitch and roll angle error through the coupling relationship of IMU three-axis attitude. The pitch and roll error observations were built by using the difference between the pitch

<sup>1</sup>SIMON BÉNÉTEAU / MAGENTA FILMS, for the drone view.

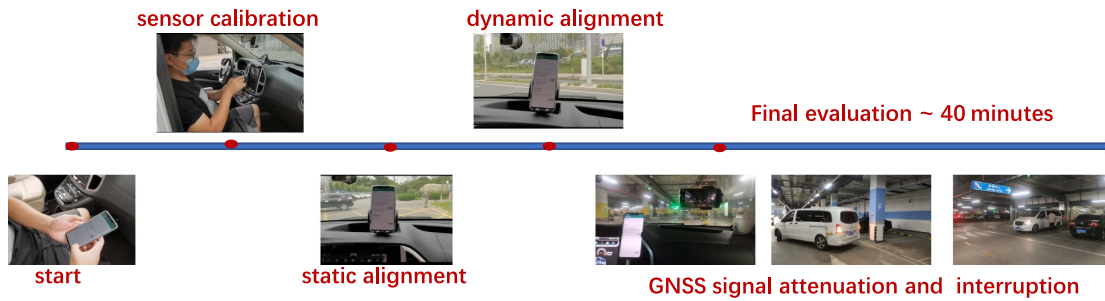


Fig. 16. Test process of track 6.

and roll angles calculated by the INS and the horizontal attitude estimated by the accelerometer output during the still phase. At the same time, the difference between the currently estimated heading angle point and the average value of the heading angle of the previous five sampling points in the still phase is used as heading angle error observation to improve heading estimation.

*c) Step 3:* Given that height error is considered in IPIN2022 competition, which is expressed as floor error, the difference between the height calculated by the barometer at the current moment and the ones at the initial time is used to obtain the relative height, for assisting in determining the floor changes.

*d) Correction model:* The escalator and elevator scenario was introduced in the IPIN2021 competition. A moving platform correction model was proposed in the system developed by Team X-lab to solve the zero-velocity false detection when the testers ride still on the escalator and elevator. The motion characteristics of the escalators and elevators are also taken into account to constrain the velocity error and improve the positioning accuracy in the proposed moving platform correction mode [42].

## VIII. TRACK 6: SMARTPHONE ON VEHICLE (2022)

This section describes track 6, which was based on the use of smartphones attached to a vehicle and took place in 2022.

### A. Track Description

The goal of this track is to evaluate the performance of different integrated navigation solutions based on a vehicle-mounted smartphone, which includes GNSS, accelerometer, gyroscope, and magnetometer, among other sensors. The test route includes both an outdoor scenario with an unobstructed satellite view, one with a partially obstructed view and an indoor scenario without a satellite view. The outdoor scenario with an unobstructed view accounts for 40% of the total test route and is not considered for computing the evaluation score.

The test route of track 6 (see Fig. 17) includes an outdoor scenario with an unobstructed satellite view, an attenuation scenario with a partially obstructed view and an indoor scenario without a satellite view. In the test process (see Fig. 16), there were several long interruptions of the GNSS signal and an irregular test route was adopted. Besides the navigation measurements derived from the sensors installed in the smartphone, there was no external aid information and no prior knowledge of the test



Fig. 17. Test route and GNSS condition of track 6.

route. The competitors could only rely on smartphone data to calculate the vehicle position.

### B. Environment and Measurement Setup

In this off-site track, all data for testing and scoring have been provided by the organizers before the IPIN conference. The teams in the competition can calibrate their algorithmic models with several databases that contain readings from the sensors of the smartphone mounted on the vehicle and some ground truth positions. Then, each team competes using additional database files, but in this case, they have to estimate the ground truth reference without knowing it. Moreover, to prevent the use of the map-matching method, an irregular driving route is chosen.

The raw multisensor data, which includes the information of all the signals captured by the smartphone in real-time in the vehicle scenario, was recorded using a Huawei Mate 20 smartphone. The smartphone was attached to the car dashboard throughout the test process to record the motion measurements.

The test area of track 6 is a typical urban road environment. A single test process takes about 1 h and the test route has four phases: a static initial alignment phase (about 5 min), an open environment phase (about 20 min), an obstructed environment phase where the GNSS signal is weakened or blocked by the

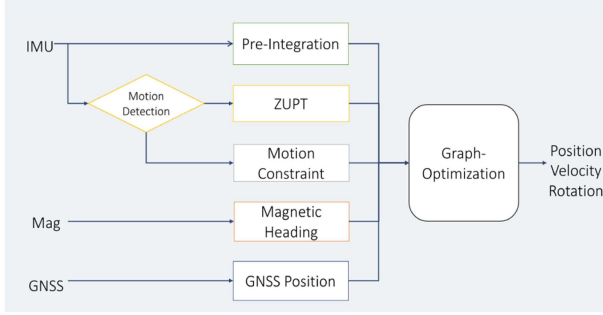


Fig. 18. Overview of adopted system.

nearby buildings or trees (about 25 min, during which the GNSS positioning results will be often disrupted), and a no GNSS signal phase (underground parking lot, about 10 min, no GNSS positioning results). The test vehicle drives in different ways, such as going straight, turning, reversing, and parking.

During the data collection phase, the same vehicle, smartphone, and smartphone installation method are used for all the testing and scoring trials. The smartphone is securely fixed to the vehicle body as shown in Fig. 16. The coordinate system of the vehicle body and the sensors are different, so the mounting angles are required.

### C. Description of Competitors (Smartphone on Vehicle)

1) *Team WHU-GD*: As shown in Fig. 18, the method uses a graph-optimization method to fuse GNSS, IMU, and magnetometer information. The GNSS provides absolute position constraints. Moreover, a magnetic field heading helps reduce heading drift in the long term. However, the GNSS signal is often disrupted in field testing, and the raw GNSS measurements are not accessible. Therefore, enhancing the relative positioning capability based on IMU with the motion model constraint is crucial. The motion model includes ZUPT and NHC.

This approach estimates the following:

- 1) the installation parameters  $R_{vb}$  and  $l^b$ , which are rotation and translation between the vehicle and body frames;
- 2)  $m^n$ , which is the magnetic field vector in the navigation frame;
- 3)  $S_i$ , which is the system state of the keyframe  $i$ .

This approach chooses the keyframe according to a fixed time interval of 1 s.

It is defined as

$$S_i = \{t_{nb_i}, R_{nb_i}, v_{nb_i}, b_i^a, b_i^g, b_i^m\} \quad (2)$$

where  $t_{nb_i}$ ,  $R_{nb_i}$ , and  $v_{nb_i}$  represent the position, rotation, and velocity of the body frame (alignment with the IMU) in the navigation frame.  $b_i^a$ ,  $b_i^g$ , and  $b_i^m$  represent biases of the accelerometer, gyroscope, and magnetometer, respectively.

The structure of the graph optimization consists of the factors shown in Fig. 19 and described as follows.

a) *Preintegration Factor*: This factor establishes the relative pose and velocity constraint between two consecutive

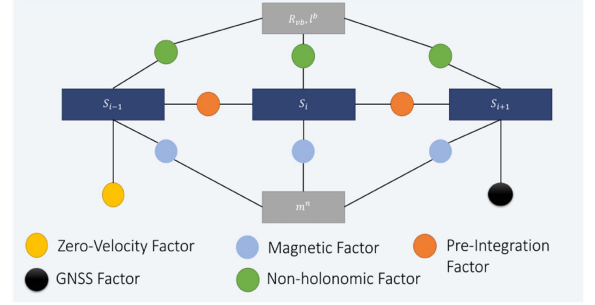


Fig. 19. Structure of the graph optimization.

keyframes. Because of the low accuracy of the built-in IMU in the mobile phone, a simplified INS mechanization is used to enhance efficiency without compromising accuracy. Specifically, the impact of the angular rate and sculling effect due to the Earth's rotation and motion speed is neglected.

b) *Zero-Velocity Factor*: ZUPT is used to reduce the accumulation of velocity errors. Because the velocity of consumer-grade IMU increases rapidly, the ZUPT is essential to improve the accuracy of the relative position when the GNSS signal is unavailable. This factor gives a prior probability to the velocity when the zero-velocity state is identified. The raw output of the IMU over a short period (2 s in this approach) is used for stationary detection.

c) *Nonholonomic Factor*: The nonholonomic factor is based on the assumption that the vertical and lateral velocities in the vehicle frame are nearly zero, because the mobile phone installation in the field testing is uncertain, the installation parameters need to be estimated online. The initial value is estimated when the velocity value is high enough. The installation parameters are updated online during the testing to prevent the impact of the installation parameters change.

d) *Magnetic Factor*: The magnetic field vector limits the absolute heading during the testing. It is important to note that the magnetic field vector is very noisy in some places, such as inside buildings or near electronic devices.

In this context, the  $\chi^2$ -test is adopted to eliminate the effect of these noise sources.

e) *GNSS Factor*: The GNSS position is the only source that can provide absolute position information in this competition, because the GNSS signal is prone to interruption or nonGaussian noise, the  $\chi^2$ -test is used to determine whether the current GNSS position is valid. Taking advantage of the flexibility of the graph-optimization architecture, the relative distance of the GNSS positions between two keyframes is used first and then the absolute position constraint after several seconds is applied. This strategy helps increase the reliability of the position of the keyframe, which is used in the  $\chi^2$ -test.

f) *General notes*: This system adopts a sliding window strategy to ensure the system can run in real-time.

The marginalization strategy is used to preserve the information from deleted keyframes.

The parameters of this approach are tuned based on the given training dataset.

## IX. TRACK 7: CIR IN WAREHOUSE

This section describes track 7, which was based on the use of CIR in warehouses and took place in 2021 and 2022.

### A. Track Description

RF positioning in cluttered indoor environments is challenging. As signals travel through the environment along different paths it is difficult to determine the correct ToF of the transmitted signals. Traditionally, fingerprinting-based solutions have been used to estimate a rough position from narrow-band signals, such as Wi-Fi or bluetooth. However, with modern UWB technology, signals can be transmitted at higher bandwidths, enabling a much higher spatial resolution from which complex propagation conditions can be extracted, such as absorption, reflection, diffraction, and scattering [43]. While UWB is progressively integrated, but not yet widely spread, into consumer devices, current progress in development and standardization makes it likely that it will be ubiquitous in the near future. This allows for low-cost ad hoc positioning.

To leverage the benefits of the high spatial resolution we can make use of the CI. For sufficiently high bandwidths the CI roughly corresponds to the complex-valued CIR. Many algorithms have been investigated that exploit the CIR to extract spatial information in order to enhance the positioning performance. They have been used for ToF error mitigation [44], which uses the CIR to estimate an environment-specific ToF error, fingerprinting [45], which exploits the raw CIR as location-specific information, and C-SLAM [46], which exploits the multipath components included in the CIR. Therefore, besides ToF estimates, we provide the raw CIRs, which allows enhancement of localization accuracy.

The challenge is divided into two parts. In the first part, the data that is used for training and testing originate from the same environment setup. In the second part, we made some changes to the environment setup (i.e., we moved mobile metallic objects) in order to consider the robustness of the algorithms to environmental changes. For the second scenario, we do not provide training data but only test data. The trajectories we use for testing in the second scenario stay within a similar area as the one used in the first scenario.

In 2022, we investigated the generalization to a different agent for collecting data. In a typical industrial application setting, data points are easily collected and labelled by automated guided vehicles, but the tracking targets can be other agents, such as persons. The different agents have various influences on the signal, due to the shadowing of, e.g., a person or reflections of a robot. Also, movement patterns and height of the radio unit are different, which might also influence the performance. The majority of the provided data for the validation and training are collected by a mobile robot, while the evaluation is based on the tracking of a worker in an industrial setting.

In both years the ground truth of the transmitter positions is collected using a millimeter-accurate Qualisys motion tracking system. The data are collected and synchronized by an NTP server and preprocessed (corrupted data points are removed and RF and positioning reference data are synchronized).

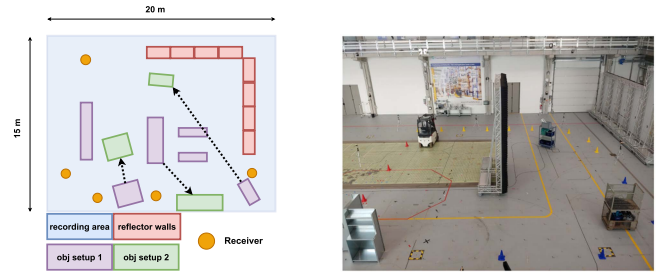


Fig. 20. Schematic environment setup, including exemplary object setups 1 and 2 (left-hand side) and a similar real-world environment (right-hand side).

### B. Environment and Measurement Setup (2021)

The environment consists of an area of  $\approx 300 \text{ m}^2$ , partially enclosed by reflecting walls (consisting of the walls of the measurement wall, including metal gates and artificially included reflector/absorber walls elements) and various metal objects that are typical of industrial indoor environments like, e.g., industrial vehicles or metal shelves. Fig. 20 (left-hand side) schematically sketches the environment, while the real-world environment is shown on the right-hand side. The receiving anchors are placed around the recording area at about 1.5 m height. The transmitter device is carried by a human/worker and regularly transmits UWB signals received by the anchors. The data are recorded using a platform based on the Decawave DW1000 UWB chip with a centre frequency of 4 GHz and 499.2 MHz bandwidth.

This challenge contains the following two scenarios.

- 1) For the first scenario a training dataset with ground truth positional information is provided; the models submitted by the competitors are evaluated on a test set (a few trajectories) that originates from the same measurement campaign, i.e., training and test datasets were recorded on the same environmental setup. Both training and test datasets contain complete trajectories while the trajectories of the test dataset are shorter. The testset does not contain ground truth position labels.
- 2) The second scenario presents a modification of the first scenario. In this setup, clutter elements within the environment (e.g., forklift, van, etc.) were moved, which led to a slightly different propagation scenario. The goal of this scenario is to test if the models submitted by the competitors overfit the previous environmental setup and fail to generalize well to changes to the environment. Therefore, the training dataset does not include any trajectory collected within this modified scenario, which is only considered in the trajectories within the testset.

### C. Environment and Measurement Setup (2022)

The environment consists of a warehouse area of  $\approx 1200 \text{ m}^2$  partially enclosed by reflecting walls (consisting of the walls of the warehouse, including metal gates). The environment contains various metal objects (e.g., industrial vehicles or metal shelves). Fig. 21 shows a picture of a part of the warehouse. Receiving anchors are placed around the recording area at about





Fig. 21. Image of the environment. The mobile robot can be seen on the right.

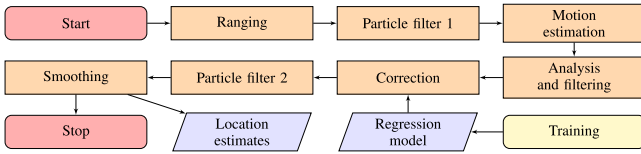


Fig. 22. Flowchart of the imec-WAVES localization approach. Each rectangular box represents a step in the process. Training the regression model for range error correction is done separately.

1.5 m height. The transmitter device is carried by the mobile agent/tracking target and regularly transmits UWB signals received by the anchors. In the data collection phase, it is attached to a mobile robot. In the evaluation phase, it is carried as a handheld by a human/worker. An exemplary and representative evaluation/experiment dataset for adjusting models was provided.

#### D. Description of Competitors (CIR in Warehouse)

1) *Team imec-WAVES (2021)*: imec-WAVES' localization solution's core is

- 1) distance estimation between each tag and anchor,
- 2) range correction through a regression model, and
- 3) a PF for localization.

Fig. 22 shows the individual steps of the system. A custom ranging algorithm provides range estimates for each captured CIR. A first pass of a PF provides an initial approximation of the user's location throughout time, from which their motion trajectory is calculated. Erroneous range estimates are identified by examining time-range plots for each tag–anchor pair. At this stage, a set of predictors serves as input for the regression model. The regression outputs a scalar distance correction that is applied to the original range estimate. In training, this reduced the MAE from 24 down to 3 cm (excluding uncorrectable estimates). A second PF utilizes the updated range estimates to obtain a better location estimate. Finally, a smoothing step in conjunction with position interpolation predicts the location at each requested timestamp.

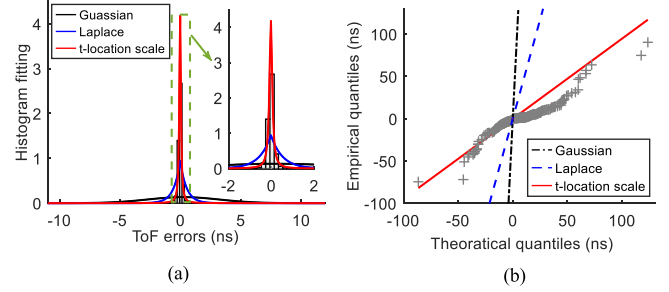


Fig. 23. (a) Normalized histogram fitting of the ToF estimation errors and (b) the QQ plots.

a) *Ranging algorithm*: This solution calculates range or ToF using a threshold-based algorithm. The threshold is calculated from the noise, which is determined heuristically after partitioning the CIR into a noise region, a region-of-interest which contains the first path component, and a region with only multipath components and noise.

b) *Regression model*: The correction model uses Gaussian process regression with a constant basis function and exponential kernel. Training is performed with fivefold cross-validation to reduce the risk of overfitting. Predictors are calculated from the following.

- 1) The original CIR measurement (anchor number, first path bin power, maximum bin power, and distance estimate).
- 2) The location estimate [AoD from the anchor and compatibility with distance estimate].
- 3) The motion trajectory [velocity, direction, turning rate, and angle-of-arrival (AoA) on the tag].

c) *Tracking*: In this competition, tracking was leveraged to the PF algorithm, which has better accuracy than the Kalman-framework filters generally [47]. In this competition, only the 2-D coordinates  $\mathbf{P}_{\text{MU}}$  of the moving user (MU) are considered, which are updated via the constant velocity motion model, given as follows [48]:

$$\begin{bmatrix} \mathbf{P}_{\text{MU}}^{(t+1)} \\ \mathbf{v}_{\text{MU}}^{(t+1)} \end{bmatrix} = \begin{bmatrix} \mathbf{I}_2 & \Delta t \cdot \mathbf{I}_2 \\ \mathbf{0} & \mathbf{I}_2 \end{bmatrix} \begin{bmatrix} \mathbf{P}_{\text{MU}}^{(t)} \\ \mathbf{v}_{\text{MU}}^{(t)} \end{bmatrix} + \begin{bmatrix} \Delta t \cdot \mathbf{1}_{2 \times 1} \\ \mathbf{1}_{2 \times 1} \end{bmatrix} n_v \quad (3)$$

where  $\mathbf{v}_{\text{MU}}$  denotes the 2-D velocity of the MU,  $\Delta t$  the time difference between timestamps  $t$  and  $t + 1$ .  $n_v$  represents the Gaussian velocity errors. In total, 1000 particles were utilized to generate the proposed likelihood of the MU locations within the targeted area. The weights were updated via the PDF of the ToF estimation errors.

However, in the case of NLOS propagation, the ToF estimates may have large offsets due to the wrong threshold judgment. To better quantify the ToF statistical error, its histogram was fitted on three widely-used distributions, namely, Gaussian, Laplace, and t location-scale distributions [49]. Fig. 23 shows the histogram fitting on these three distributions and their goodness-of-fit via QQ plots. Benefiting from handling with heavier tails, t location-scale distribution presents the most straight line in QQ plots, which illustrates that the ToF estimation errors best follow t location-scale distribution.

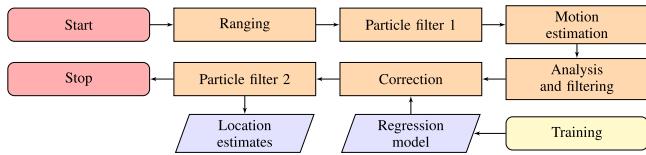


Fig. 24. Flowchart of the imec-WAVES localization approach. Each rectangular box represents a step in the process. Training the regression model for range error correction is done separately.

The same implementation and parameters are used in both instances of the PF in the systems developed by team imec-WAVES.

2) *Team imec-WAVES (2022)*: In 2022, the localization solution’s core remains similar to the approach used by Team imec-WAVES during the IPIN 2021 competition. The main difference was that in 2021 the EvaalAPI interface was not used, so the solution presented in 2022 by imec-WAVES was real-time.

It consists of the following.

- 1) Distance estimation between each tag and anchor.
- 2) Range correction through a regression model.
- 3) Two instances of a PF for localization.

Fig. 24 shows the individual steps of the system. A custom ranging algorithm provides range estimates for each captured CIR. A first pass of a PF provides an initial approximation of the user’s location throughout time, from which their motion trajectory is calculated. A set of predictors serves as input for the regression model. The regression outputs a scalar distance correction that is applied to the original range estimate. A second, final PF utilizes the updated range estimates to obtain a better location estimate. The location estimate at each requested timestamp is calculated by using the prediction step of the final PF.

a) *Ranging algorithm*: A threshold-based algorithm is used to calculate range or ToF. The threshold is calculated from the noise, which is determined heuristically after partitioning the CIR into a noise region, a region of interest which contains the first path component, and a region with only multipath components and noise. Algorithm parameters are obtained through the optimization of the training data. A fixed bias correction term is obtained from the median ranging error of each anchor’s training data range estimates. The term is subtracted immediately after the ranging step. Negative range results are dropped. Previous range estimations are not used.

b) *Regression model*: The correction model uses Gaussian process regression with a constant basis function and a Matern 5/2 kernel. Training is performed with fivefold cross-validation to reduce overfitting. Predictors are calculated from the following.

- 1) The original CIR measurement (anchor number, first path bin power and maximum bin power).
- 2) The location estimate (AoD from the anchor, compatibility with distance estimate,  $X$ - and  $Y$ -coordinates).
- 3) The motion trajectory (velocity, direction, and AoA on the tag).

Due to the real-time character of the data in 2022, trajectory estimation was much harder. In fact, predictors used in 2021,

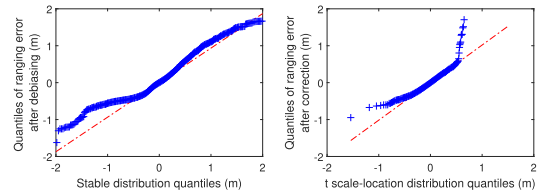


Fig. 25. QQ plot of the measurement likelihood functions that are used in the first and second PF. The first filter incorporates a function based on a Stable distribution fitted to unbiased ranging error. The second filter makes use of a  $t$  location-scale distribution fitted to the ranging error after it is corrected by the regression model.

such as turning rate, proved too unreliable this time around. Furthermore, the regression model could only be trained with data that contained global timestamps, as these timestamps are needed to calculate the motion trajectory. This made the largest available set of training data not applicable for training this model.

c) *Tracking*: PF algorithm was used to track the agent. Only the  $X$ - and  $Y$ -coordinates of the MU are considered. The particles are updated through a constant velocity motion model, using nonadditive process noise. The first PF contains 700 particles, with a measurement noise of 0.17 m and a process noise of  $10 \text{ ms}^{-2}$ . The second PF contains 2000 particles, with a measurement noise of 0.02 m and a process noise of  $15 \text{ ms}^{-2}$ . The measurement likelihood function to update the particles makes use of a PDF fitted to the range estimation errors from the training data. Fig. 25 shows the QQ plot of each distribution fit. For the first filter, the PDF is fitted using a stable distribution on the debiased estimates. In the second filter, a  $t$  location-scale distribution is fitted to the ranges after correction of the regression model.

3) *Team SPSC*: Team SPSC used a two-step method similar to the algorithm presented in [50], [51]. First, a snapshot-based parametric channel estimation and detection algorithm extracts delays and corresponding amplitudes of multipath signal components out of the received baseband signal. Second, a sequential estimation algorithm estimates the state of the mobile agent by using the delays and amplitudes as measurements. More specifically, the sequential estimation algorithm jointly performs probabilistic data association and estimation of the mobile agent state together with all relevant model parameters, employing the SPA on a factor graph. It adapts in an online manner the time-varying component SNR as well as the detection probability of the LOS component. The concept of probabilistic data association, together with adaptation of the LOS detection probability, enables the algorithm to solve the nonlinear positioning problem and mitigate NLOS situations, while still offering an execution time in the magnitude order of milliseconds. In the following, the probabilistic system model of Team SPSC’s algorithm is briefly discussed.

a) *Channel Estimation and Detection Algorithm*: The channel estimation and detection algorithm presented in [51, Supplementary Material] was applied to the baseband signal vector at each time  $n$  and for each anchor  $j$  independently. It provides a measurement vector  $z_n^{(j)}$  containing a number of

$M_n^{(j)}$  measurements  $\mathbf{z}_{m,n}^{(j)} = [\hat{d}_{n,m}^{(j)} \hat{u}_{n,m}^{(j)}]^T$ . Each  $\mathbf{z}_{m,n}^{(j)}$  contains a distance measurement  $\hat{d}_{n,m}^{(j)}$ , and a normalized amplitude measurement  $\hat{u}_{n,m}^{(j)}$ .

### b) SPA-based Sequential Estimation Algorithm:

The components of the measurement vector  $\mathbf{z}_n^{(j)}$  are subject to data association uncertainty, i.e., it is not known which measurement originates from the LOS, from multipath or from a false-alarm. Based on the concept of probabilistic data association, an association variable is defined as

$$a_n^{(j)} = \begin{cases} m \in \{1 \dots M_n^{(j)}\}, & \mathbf{z}_{n,m}^{(j)} \text{ is the LOS meas. in } \mathbf{z}_n^{(j)} \\ 0, & \text{there is no LOS meas. in } \mathbf{z}_n^{(j)}. \end{cases} \quad (4)$$

It differentiates between the conditional likelihood functions for LOS and NLOS measurements, which, for the distance measurements  $\hat{d}_{n,m}^{(j)}$  are given as a Gaussian PDF with mean value that is geometrically related to the agent position  $\mathbf{p}_n$  and a uniform PDF, respectively. The system jointly performs sequential estimation of amplitude states  $u_n^{(j)}$ , which are assumed to be independent per anchor. The corresponding conditional amplitude likelihood functions are given as Rician PDF and Rayleigh PDF for LOS or NLOS measurements, respectively. The LOS detection probability, which occurs as part of the data association prior and represents the probability that there is a LOS component per time step and anchor, is modeled as the product  $p_D(u_n^j) q_n^{(j)}$ , between the amplitude-related detection probability  $p_D(u_n^j)$  and a prior LOS probability  $q_n^{(j)}$ . The latter is modeled discretely, as a first-order Markov process. The likelihood functions, together with the prior PDF of the data association variable, define the joint pseudolikelihood function  $\tilde{g}_z(\mathbf{z}_n^{(j)}; \mathbf{p}_n, u_n^{(j)}, a_n^{(j)}, q_n^{(j)})$ .

The agent state is described by the state vector  $\mathbf{x}_n = [\mathbf{p}_n^T \mathbf{v}_n^T]^T$ , which is composed of the 2-D agent position  $\mathbf{p}_n$  and velocity  $\mathbf{v}_n$ . The agent motion, i.e., the state transition PDF  $\Upsilon(\mathbf{x}_n | \mathbf{x}_{n-1})$ , is modeled by a linear, constant velocity, and stochastic acceleration model with standard deviation set to 1/3 of the mean step width of the mobile agent. The state transition PDF of the normalized amplitudes  $\Phi(u_n^{(j)} | u_{n-1}^{(j)})$  is modeled as a Gaussian distribution with standard deviation set to 5% of the last amplitude estimate. The elements of the first-order Markov transition matrix  $\Psi(q_n^{(j)} = \omega_i | q_{n-1}^{(j)} = \omega_k)$ , as well as the initial distributions, i.e.,  $f(\mathbf{x}_0) p(q_0^{(j)}) f(u_0^{(j)})$ , were initialized heuristically as described in [50].

By applying Bayes' rule as well as some commonly used independence assumptions, the factorized joint posterior PDF is computed, which is visually represented by the factor graph shown in Fig. 26.

The agent state is estimated as the minimum mean-squared error estimate given as

$$\hat{\mathbf{x}}_n^{\text{MMSE}} \triangleq \int \mathbf{x}_n f(\mathbf{x}_n | \mathbf{z}) d\mathbf{x}_n. \quad (5)$$

In order to obtain (5) the marginal posterior PDF is calculated by performing message passing on the factor graph in Fig. 26

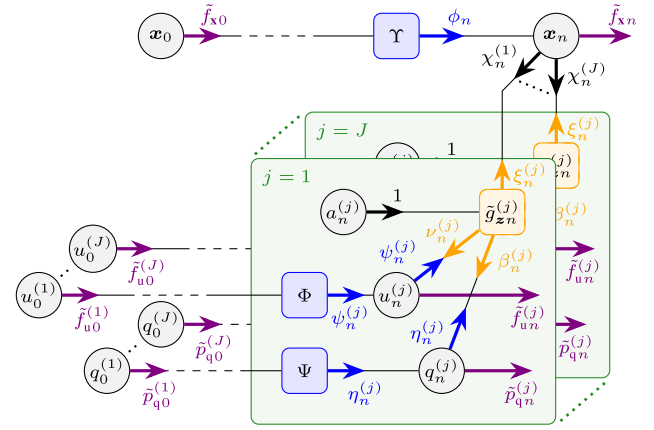


Fig. 26. Factor graph representing the factorization of the joint posterior PDF and the messages according to the SPA. See [50] for further details.

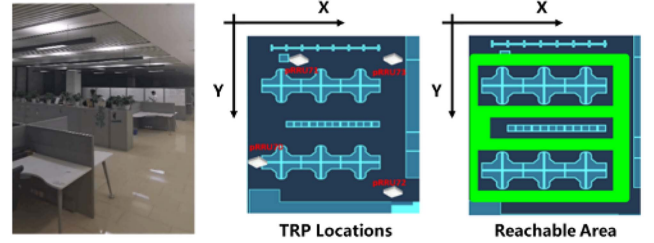


Fig. 27. Measurement environments.

utilizing the SPA rules. Since the integrals involved in the calculations of the messages cannot be obtained analytically, a sequential particle-based implementation is used.

## X. TRACK 8: 5G IN OPEN-PLAN OFFICE (2022)

This section describes track 8, which was based on 5G in an open-plan office and took place in 2022.

### A. Track Description

Track 8 was dedicated to 5G positioning based on UL-TDOA, which is widely adopted in 5G products. 2022 was the first time such technology was part of an IPIN competition.

The Huawei 5G system is deployed in an indoor office in the Huawei–Chengdu building. The area is about 15 m × 15 m with ceiling height of 3.2 m. There are working tables, chairs, and partition panels in the room with heights in the 0.5–1.5 range. Four pRRUs with known locations are mounted on the ceiling, see Fig. 27. The UE is a Huawei Mate 30 Pro terminal. The UE transmits in bursts of 80 ms. The pRRUs detects the received SRS and calculates the positioning measurements, such as RTOA and RSRP. The UE was fixed onto a trolley with a constant height of 1.2 m, and the UE moves at a speed of 0.2–0.5 ms<sup>-1</sup> within the reachable area (highlighted in green colour). During the walking route, the UE signals to some TRPs might be blocked by tables, partition panels and shelves. The tables and panels are made of plywood (2–4 cm thick), and the shelves are made of sheet metal. Hence, there may exist a mixture of LOS, near LOS,

**TABLE V**  
 COORDINATES OF THE PRRUS

ID	X (m)	Y (m)	Z (m)
0	1.75	20.2	3.2
1	4.85	11.25	3.2
2	12.48	21.85	3.2
3	9.75	12.48	3.2

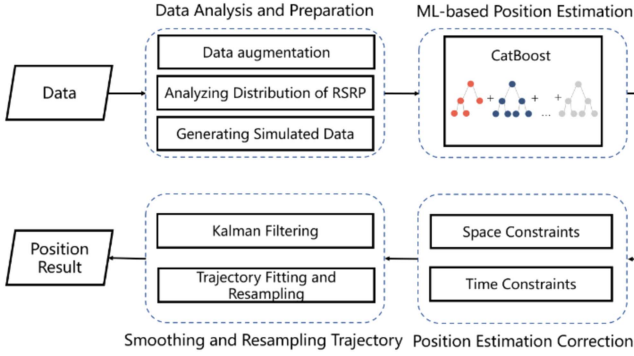


Fig. 28. Pipeline of team mobile's solution.

and NLOS channels. Strong multipath effects may also exist due to reflections from the environment, such as concrete walls, columns, and other metallic objects.

Four sets of data are given, named *Testing\_A*, *Testing\_B*, *Scoring\_A*, and *Scoring\_B*. Each set contains 1000 measurements ( $\approx 85$  s long) with 50 ground truth positions. Ground truth positions are only given for the testing sets. The RTOAs is measured by using the MUSIC algorithm with a known accuracy of 1 ns tested in a LOS environment. There are existing timing errors among the receivers in TRPs, called TAE. The TAEs of the TRPs are unknown, but should be in the  $-100$  to  $10$  ns range.

The coordinates of the pRRUs's locations are given in Table V. The ground truth coordinates of pRRUs3 are actually (12.48 and 9.75 m), that is, the  $xy$  coordinates are exchanged with each other. This is to introduce a coordinate error, which might happen in practice.

1) *Competition Area*: For IPIN 2022, due to movement restrictions, the data set of track 8 was collected only from one indoor office instead of two independent indoor scenarios as planned. Fortunately, the measured office has diverse furniture and facilities, which enable diverse channels in different locations, such as strong LOS, near LOS, and NLOS. Four datasets are measured in the office, and their routines are different in time. Competitors were encouraged to develop self-localization for UL-TDOA including TAE estimation and pRRUs selection, possibly using artificial intelligence.

## B. Description of Competitors (5G in Open-Plan Office)

1) *Team Mobile*: The technical route used by 1) mobile team is mainly based on an ML approach. Fig. 28 shows the pipeline of team mobile's proposed solution. First, simulated data is generated based on data statistics for the purpose of data augmentation, the training data set is built and then CatBoost [52] is used to complete the end-to-end positioning task. Then the

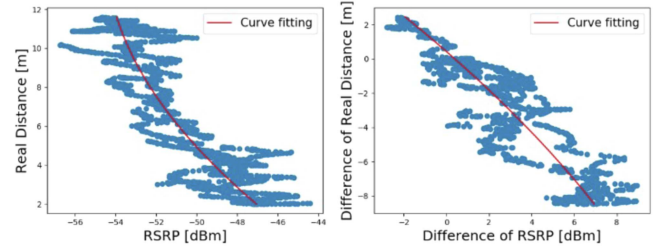


Fig. 29. (a) Relationship between the RSRP received by pRRU0 and the real distance. (b) Relationship between the difference of RSRP and the real distance difference of pRRU0 and pRRU1.

position estimation is further corrected based on the room layout and spatio-temporal continuity of the trajectory. Finally, KF is used to smooth the trajectory and resample it in real-time.

a) *Data Analysis and Preparation*: The data provided by Track 8 include the timestamps and eight features which are the RTOA and RSRP estimated by the four pRRUs. Note that there are timing errors among the receivers in pRRUs, called TAEs. The unknown TAEs greatly affects the accuracy of TOAs and the position estimation results, and it is also time-varying among different datasets. In contrast, RSRP is more stable because data in all data sets are collected in the same environment. In this case, the solution provided by Team Mobile identifies the RSRP as the key feature.

To fully capture the RSRP feature, an ML-based approach is planned to be used in order to derive the user position. However, the labeled dataset provided by track 8 is too small. Thus, an interpolation method is applied to augment the labeled data. Then, the relationship between the RSRP received by each pRRU and the distance in the real data are quantified. Also, the relationship between the RSRP difference and the real distance difference of each pRRUs is evaluated. As shown in Fig. 29, both are negatively correlated.

Based on these relationships, the system can generate many trajectories in a simulated experimental environment and obtain the corresponding simulated RSRP. Meanwhile, the team can verify the effect of the simulation method on the real dataset. For the interpolated real trajectory in the data set of *Testing\_B*, the RSRP generated by the simulation algorithm has a similar distribution with the real RSRP, as shown in Fig. 30.

b) *Machine Learning (ML)-based Position Estimation*: When there is enough data to form the training data set, CatBoost is used to complete the end-to-end position estimation task. CatBoost is a supervised learning algorithm based on gradient boosting and has excellent performance while reducing overfitting and the time spent on tuning. The CatBoost model takes the true coordinate  $[x_t, y_t]$  as a label and the RSRP and the differences of RSRPs received by two different pRRUs as the input vector  $\text{Input}_t$  which can be represented as shown in (7)

$$\text{Input}_t = [R_0^t, \dots, R_{N-1}^t, DR_{0,1}^t, \dots, DR_{N-2,N-1}^t] \quad (6)$$

$$DR_{i,j}^t = R_i^t - R_j^t \quad (7)$$

where the  $N$  means that there are  $N$  pRRUs while  $R_{i-1}^t$  means that the RSRP received by the  $i$ th pRRUs at time  $t$ .

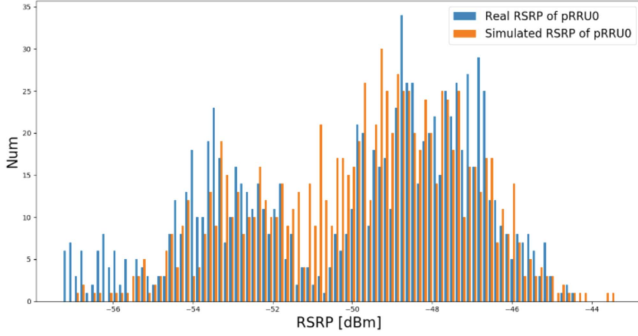


Fig. 30. Distribution of the real RSRP received by pRRU0 and the simulated RSRP of pRRU0.

*c) Position Estimation Correction:* Using CatBoost, a position based on RSRP can be estimated, however, RSRP has a large random noise that makes the estimation unstable. To achieve a more stable estimation, the system uses additional information to optimize the position estimation. For example, the users cannot pass through obstacles (e.g., furniture) because of space constraints that can be inferred from the reachable area and the trajectory in the data set. Furthermore, due to time constraints, it is unlikely that the two adjacent estimated positions are far apart. Therefore, abnormal position estimations are fixed based on the reachable area, historical position information, and motion direction.

*d) Smoothing and Resampling Trajectory:* With these data processing methods, reliable and stable position estimation can be reached. However, the normal trajectory should be smooth and continuous. Therefore, a KF is used to smooth the trajectory in real-time. Then, the relationship between the recent time and the estimated position is fit and resampled to obtain the results required by the competition.

*2) Team TX8:* In the IPIN 2022 competition track 8, two sets of data are given to calibrate the algorithmic models. In each dataset, the TOA and RSRP measurements are provided. As already identified by team mobile, high precision positioning requires estimating the TAEs accurately, i.e., to get the unknown timing errors among the receivers in TRPs. In addition, since the indoor environment is very complex, there exists a mixture of LOS paths, weak LOS paths, NLOS paths, causing a lot of outliers in the TOA and RSRP measurements. To achieve high-precision positioning, the outliers must be handled reasonably. For the TAEs estimation, the RSRP measurements are employed. Generally, the RSRP can be expressed as follows:

$$\sigma = A - 10\eta \log(d) + \varepsilon(1) \quad (8)$$

where  $\sigma$  is the RSRP measurement,  $d$  is the distance between the terminal and TRP,  $A$  and  $\eta$  are the model parameters, which can be determined by using the datasets, and  $\varepsilon$  is the measurement noise. In this manuscript, a Bayesian filter is employed to estimate the TAEs and the location of the terminal simultaneously. The state space model for the TAEs and location estimation can be written as [53]

$$\mathbf{x}_k = \mathbf{F}_{k-1}\mathbf{x}_{k-1} + \mathbf{G}_{k-1}\mathbf{w}_{k-1} \quad (9)$$

$$\mathbf{z}_k = \mathbf{h}(\mathbf{x}_k) + \mathbf{v}_k \quad (10)$$

$$\mathbf{F}_{k-1} = \begin{bmatrix} 1 & T & 0 & 0 & 0 & 0 & 0 \\ 0 & 1 & 0 & 0 & 0 & 0 & 0 \\ 0 & 0 & 1 & T & 0 & 0 & 0 \\ 0 & 0 & 0 & 1 & 0 & 0 & 0 \\ 0 & 0 & 0 & 0 & 1 & 0 & 0 \\ 0 & 0 & 0 & 0 & 0 & 1 & 0 \\ 0 & 0 & 0 & 0 & 0 & 0 & 1 \end{bmatrix} \quad (11)$$

$$\mathbf{G}_{k-1} = \begin{bmatrix} \frac{T^2}{2} & 0 & 0 & 0 & 0 \\ T & 0 & 0 & 0 & 0 \\ 0 & \frac{T^2}{2} & 0 & 0 & 0 \\ 0 & T & 0 & 0 & 0 \\ 0 & 0 & 1 & 0 & 0 \\ 0 & 0 & 0 & 1 & 0 \\ 0 & 0 & 0 & 0 & 1 \end{bmatrix} \quad (12)$$

$$\mathbf{h}(\mathbf{x}_k) = [h_1(\mathbf{x}_k) \cdots h_3(\mathbf{x}_k)g_0(\mathbf{x}_k) \cdots g_3(\mathbf{x}_k)] \quad (13)$$

$$h_i(\mathbf{x}_k) = d_{i,k} - d_{0,k} + b_i, k \quad (14)$$

$$g_i(\mathbf{x}_k) = A_i - 10\eta_i \log(d_{i,k}) \quad (15)$$

$$d_{i,k} = \sqrt{(x_k - x_{\text{TRP}i})^2 + (y_k - y_{\text{TRP}i})^2} + 4 \quad (16)$$

where  $\mathbf{x}_k = [x_k \ v_{x,k} \ y_k \ v_{y,k} \ b_{1,k} \ b_{2,k} \ b_{3,k}]^T$ ,  $x_k$  and  $y_k$  are the horizontal coordinates of the terminal at time  $k$ ,  $v_{x,k}$ , and  $v_{y,k}$  are the horizontal velocities of the terminal at time  $k$ ,  $b_{1,k}$ ,  $b_{2,k}$ , and  $b_{3,k}$  are the TAEs of the TRPs at time  $k$ ,  $\mathbf{w}_{k-1}$  is the process noise at time  $k-1$ ,  $T$  is the sampling interval,  $\mathbf{z}_k = [\gamma_{1,k} \ \gamma_{2,k} \ \gamma_{3,k} \ \rho_{0,k} \ \rho_{1,k} \ \rho_{2,k} \ \rho_{3,k}]$ ,  $\gamma_{i,k}$  is the difference of the TOA measurements of TRP $i$  and TRP $0$ ,  $\rho_{i,k}$  is the RSRP measurement of TRP $i$  at time  $k$ ,  $x_{\text{TRP}i}$  and  $y_{\text{TRP}i}$  are the horizontal coordinates of the TRP $i$ ,  $A_i$  and  $\eta_i$  are the model parameters of the TRP $i$ ,  $\mathbf{v}_k$  is the measurement noise at time  $k$ .

Considering the outliers in the measurements,  $\mathbf{v}_k$  is modeled as a heavy-tailed non-Gaussian noise. Since the MCC-based EKF can handle the heavy-tailed non-Gaussian noise by using a robust cost function [54], the MCC-based EKF is utilized to estimate the TAEs and the location of the terminal based on the state space model proposed above. The workflow of the developed algorithm is shown in Fig. 31.

*3) Team DYS-BUPT:* In recent years, the DYS-BUPT team has been committed to 5G indoor positioning research to meet the positioning needs under different indoor scenes. In track 8, for the positioning scheme in the indoor office scene, DYS-BUPT solution mainly includes three parts and the system block diagram is shown in Fig. 32.

*a) Neural network regression position:* In the data enhancement part, in order to increase the amount of data for model training and improve the generalization ability of the model, neural networks are used to fit the wireless channel propagation model, so as to systematically generate more training samples to expand the training dataset, as shown in Fig. 33.

In the later position settlement part, considering that the data are RSRP collected along the continuous motion, the single point

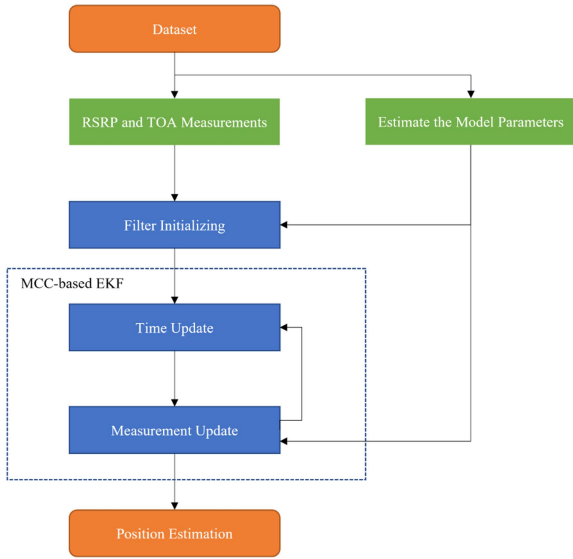


Fig. 31. Workflow of the developed algorithm.

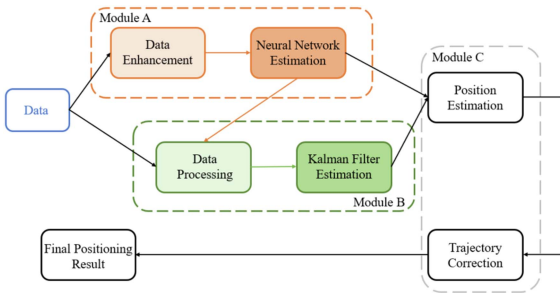


Fig. 32. System block diagram of indoor positioning scheme.

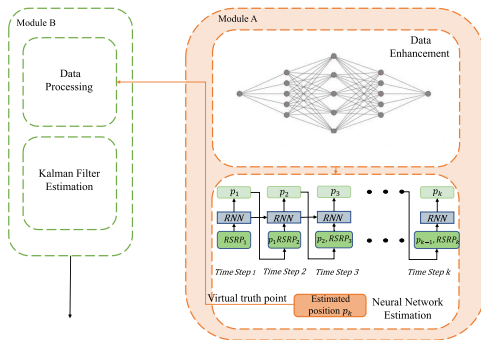


Fig. 33. Module A system block diagram.

matching method may cause a large positioning error. The position of the dynamic target is constrained by space and time, so a recursive neural network is adopted. This network is no longer like the traditional fingerprint positioning, which only relies on the fingerprint of a certain point to locate each time. Instead, it takes into account the correlation of RSRP measurements in the continuous trajectory, considers the space and time constraints of the motion trajectory on the basis of single point matching, realizes the correlation of time and location information of RSRP

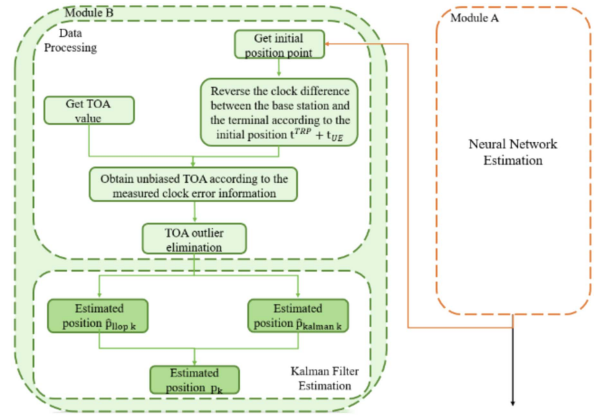


Fig. 34. Module B system block diagram.

in the trajectory, and transforms discrete positioning tasks into continuous time series feature discovery tasks.

*b) KF fusion position:* In the part of data processing, the clock error between TRP and UE is calculated based on the first point given in the regression model and the TOA information collected and then obtain unbiased TOA data based on the clock error and the original TOA. Finally, according to  $3 \cdot \sigma$  The criterion filters the data and smooths the abnormal value TOA, as shown in Fig. 34.

In the data solution part, the position at the previous time is fused with the data collected at this time through Kalman filtering to obtain the Kalman location estimation at time  $k$ . At the same time, the system obtains the LLOP estimation value at time  $k$  by solving the LLOP algorithm, and combines the two positioning methods with empirical weighting to obtain the positioning estimation value of Module B.

*c) Numerical weighted fusion and trajectory correction:* In module C, the location estimates obtained from modules A and B are empirically weighted to achieve better results. Then, consider the actual situation, and calibrate the areas that cannot be reached by pedestrians, such as points outside the room, to obtain more reliable results.

## XI. RESULTS

In this section, we report the overall scores for each track and its competitors in editions 2021 and 2022 of the IPIN Competition. Table VI presents the results for the 2021 edition, while Table VII presents the results for the 2022 edition. In both editions, as usual in the IPIN competition, the reported results correspond to the third quartile of the error metric, which is the 2-D positioning error plus a floor penalty of 15 m. Each track defined a cutoff threshold to be eligible for a prize. i.e., teams providing an error larger than the cutoff were not awarded a prize. Given the large errors provided by some teams in 2021, very large errors were reported differently in 2022. For the 2022 edition, the errors larger than three times the cutoff value are represented by  $> 3 \times 15$  in tracks 3 and 4, and by  $> 3 \times 40$  in track 6.

TABLE VI  
RESULTS 2021

Track 3: smartphone [see Section VI]		
1	GD-WHU	4.4 m
2	imec-WAVES	7.9 m
3	SCU	67.8 m
4	XMU	153.0 m
Track 4: Foot-mounted IMU [see Section VII]		
1	ICT-BUPT	61.9 m
2	Silk-Road Reckoners	4562.0 m
		54.1* m
Track 7: CIR in warehouse [see Section IX]		
1	imec-WAVES	0.09 m
1	ISCAS	0.09 m
3	SPSC	0.16 m
4	CUMT	0.16 m
5	IDLab	0.62 m
6	UT_PS	0.69 m
7	YAI	1.70 m

\* unbiased results postprocessed by track chair

TABLE VII  
RESULTS 2022

Track 2: Camera [see Section V]		
1	CamLoc	2.1 m
2	SZUSCRI	3.2 m
Track 3: Smartphone [see Section VI]		
1	X-lab	30.1 m
2	Leviathan	39.8 m
3	DYS-BUPT	> 3 * 15 m
4	imec-WAVES	> 3 * 15 m
5	XMU-ATR	> 3 * 15 m
-	BUPT-ICT	-
-	IOT2US	-
Track 4: Foot-mounted IMU [see Section VII]		
-	SmartFoot	> 3 * 15 m
-	X-lab	> 3 * 15 m
-	Leviathan	> 3 * 15 m
-	CETC54-smart hardware	> 3 * 15 m
Track 6: Smartphone on vehicle [see Section VIII]		
1	WHU-GD	14.7 m
2	team708	22.3 m
-	Leviathan	> 3 * 40m
-	ict	-
Track 7: CIR in warehouse [see Section IX]		
1	ISCAS	0.2 m
1	imec-WAVES	0.2 m
3	WHU CIRpos	0.5 m
4	CUMT-CS	1.1 m
-	LGD	-
Track 8: 5G in open-plan office [see Section X]		
1	Mobile	0.8 m
2	DYS-BUPT	0.9 m
3	TX8	4.1 m
4	WHU-UNIP	4.2 m

Table VIII gives the main techniques used in the systems described within this manuscript, where inertial techniques (PDR or PDR with ZUPT) are used by all teams in tracks 3, 4, and 6. Fingerprinting is also used by smartphone-based positioning, using only Wi-Fi, BLE, or the combination of both signals and magnetic field. Floor estimation exploits barometer information.

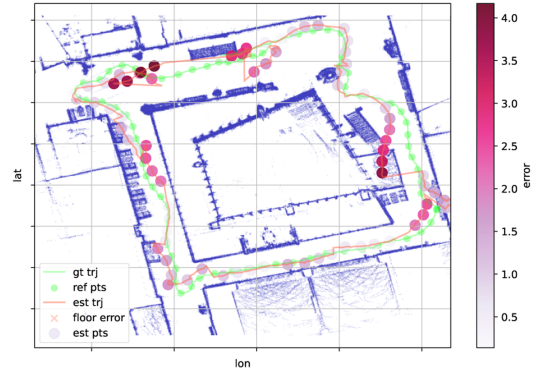


Fig. 35. Trajectory plot of track 2 winner's best scoring trial. The estimated trajectory (est trj) is evaluated against the ground truth trajectory (gt trj) at predefined reference points (ref pts) based on horizontal Euclidean distances to the corresponding estimated points (est pts) with an additional penalty for incorrectly estimated floor (marked with floor error).

As far as algorithms are regarded, a PF is used in Tracks 3 and 7. It is combined with map information. However, some teams also used environmental information without combining it with PFs, see the description of teams X-LAB and WHU-GD.

Another important element from the table is that some teams participated in more than one track: X-LAB and imec-WAVES, although they use different techniques in different Tracks.

Thus, we see from the table that the tracks created correspond to different solutions and there is little overlap among different tracks. The most overlap is among tracks 3 and 4, however, they are physically very different: track 3 is based on smartphones that can exploit the combination of data provided by low accurate built-in sensors of different nature; and track 4 is solely based on a higher-quality IMU, which enables the integration of better inertial information in the navigation algorithms.

KF and its variants are used in tracks 3, 7, and 8.

#### A. Track 2

Two teams participated in Track 2 competition: *team1* was SZUSCRI from Shenzhen University and Smart City Research Institute; *team2* was CamLoc from Beijing University of Posts and Telecommunications.

During scoring trials, the competitors connected to the testing server and started receiving testing images and returning back pose estimations. Each subsequent image was sent only after receiving the pose estimation of the previous image. The competitors had no indication of which images were to be used as reference points.

At the end of the scoring trial, the reference points were used to calculate position errors as a sum of two terms: a position error calculated from the Euclidean (horizontal) distance between the estimated position and the corresponding ground truth and a floor error penalty of 15 m. The third quartile error of the best scoring trial for each team was 3.2 m for team SZUSCRI and 2.1 m for team CamLoc (see Table VII Track 2: Camera). The trajectory of the scoring trial for the winner CamLoc is shown in Fig. 35.

TABLE VIII  
MAIN TECHNIQUES USED BY THE TEAMS PROVIDING FULL DESCRIPTION

Track	Team	PDR	Fingerprinting	Bar.	KF	PF	ML	Map	Specific algorithms
2: Camera	CamLoc	—	—	—	—	—	—	—	Image retrieval/VO Patc-Net/VLAD/SuperPoint/SuperGlue
3:Smartphone	Leviathan	PDR	Wi-Fi	Yes	ESKF	PF	—	Env. floorplan	—
	imec-Waves	PDR	Wi-Fi,BLE	Yes	—	PF	WKNN/Viterbi	3D graph	WHIPP
	X-LAB	PDR	Wi-Fi,BLE,Magn	Yes	KF	—	—	Digital map	—
4:Foot-mounted IMU	X-LAB	ZUPT	—	Yes	—	—	—	—	Strap-down inertial navigation
6:Smartphone on vehicle	WHU-GD	ZUPT	—	—	—	—	—	Graph opt.	Magnetic Heading/NHC
7:CIR in Warehouse	imec-Waves	—	—	—	KF	PF	Regression	—	Ranging algorithm/ToF
	SPSC	—	—	—	—	—	—	—	Channel estimation and detection SPA-based sequential estimation CatBoost algorithm
8:5G in open plan office	Mobile	—	—	—	KF	—	—	—	—
	TX8	—	—	—	MCC-KF	—	—	—	—
	DYS-BUPT	—	—	—	KF	—	Neural Net	—	—

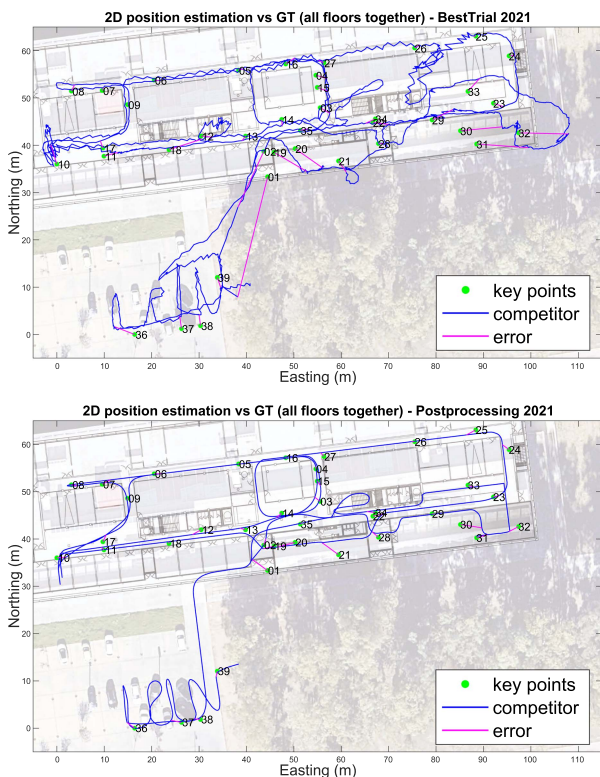


Fig. 36. Trajectory plot of track 3 (2021) best scoring trial (top) and a postprocessed trial (bottom).

B. Track 3

In 2021, a total of 16 teams registered in the competition but only four of them were able to submit the results with the EvaalAPI. This means a significant drop in participation when compared to previous editions, where 11 (2020), 12 (2019), and 13 (2018) teams submitted the results. Moreover, the best team scored an error of 4.4 m while the runner-up’s error was 7.9 m, in phase with what is expected for smartphone-based solutions according to previous on-site competitions [5]. The lower participation and the scores in 2021 reinforced the idea that the EvaalAPI was necessary to stress real-world on-site evaluation features in track 3. Fig. 36 shows the trajectory for the winner in 2021 (top plot) and the trajectory of a post-processed trajectory like in previous editions (bottom plot).

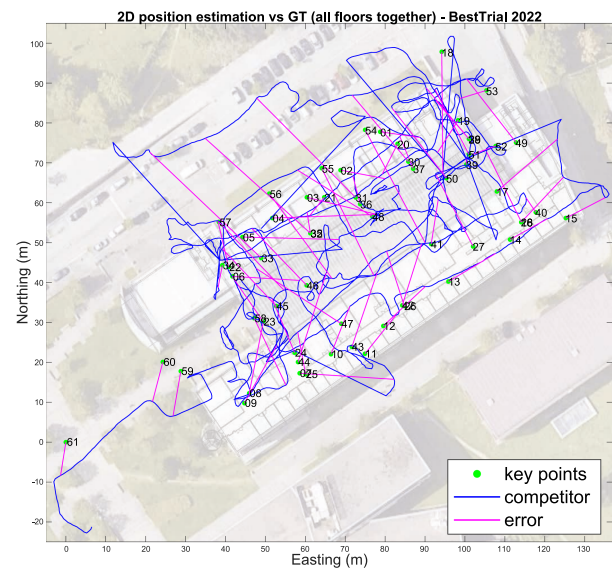


Fig. 37. Trajectory plot of track 3 (2022) best scoring trial.

In 2022, a total of ten teams registered in the competition but only seven of them were able to start the procedure to submit the results with the EvaalAPI. This means that interested teams made an effort to adopt the EvaalAPI for evaluation. The number of teams providing reliable results was in phase with the previous edition, but only two teams repeated and participated again. In this case, the best team scored an error of 30.1 m while the runner-up’s error was 39.8 m, both (of which are) above the cutoff of 15 m of track 3. Therefore none of the participating teams was eligible for the award as the overall lowest error was below the expectations for a smartphone-based positioning solution. Fig. 37 shows the trajectory for the best-performing trial in 2022, where we can observe very large positioning errors in several parts of the trajectory. The results of the other three participating teams are not shown as the errors were three times larger than the cutoff of 15 m.

In both editions, the use of advanced PF and/or KF is a core element to deal with smartphone data, including Wi-Fi fingerprinting and internal measurements. This requires properly representing the information contained in the provided floorplans. 3-D graphs are only used by one team, which seems a promising solution. In addition, the PF and KF filters need to have good



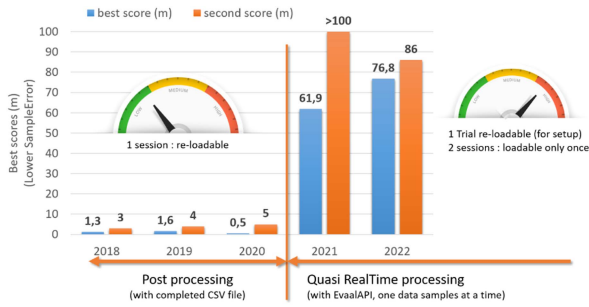


Fig. 38. Evolution of the two first scores of track 4 over the last five years.

strategies for settling the initial position and orientation as well as correcting locations in case of severe deviation.

In the 2022 edition, where the number of different devices used was higher and without BLE infrastructure supporting indoor localization, the competitors scored a positioning error much worse than usual. This even happened to the system developed by the imec-WAVES team, who has participated in the competition for many years. This highlights the relevance of having multiple heterogeneous environments to test every single solution, as a good promising indoor positioning system may not fit all environments.

Analyzing the best performing trials (see Figs. 36 and 37), we can observe that the outputs provided by the competitors are more realistic than those provided in previous editions with off-line evaluation. First, trajectories are not shown as perfectly drawn straight lines as in previous editions (see [4] and Fig. 36) as noise from sensors is visible in the trajectories as zigzag movement, drifts or messy trajectories in a challenging walking style. While short-term displacements can be captured, see text IPIN between points 35–39 in 2021 and text T3 between points 58–59 in 2022, noise and drift remain there. Second, the trajectory cannot be fixed a posteriori, so a large error in the initial location can end up in a large positioning error over the whole trajectory as it happened in 2022. Third, integration with other sources to fix the location in real-time, like map-matching may be more challenging and filters like PF and KF are computationally demanding. Those three elements can be seen in the simulated phone call of around 1 min performed in 2021 between points 25 and 26. The trajectory of the best trial is messy during the phone call, it is not fixed either in the short or in the long term, and it transverses some walls, while in a postprocessed trajectory, the trajectory between those two key points is drawn as a straight line.

### C. Track 4

In 2021, a total of three teams registered for track 4, of which only two were able to deliver results via the EvalAPI platform. This year was the first time that the EvalAPI platform was deployed for track 4. As shown in Fig. 38, there is a large gap in terms of final results before and after the introduction of the EvalAPI platform. The best score before introducing the EvalAPI platform, where full CSV files were

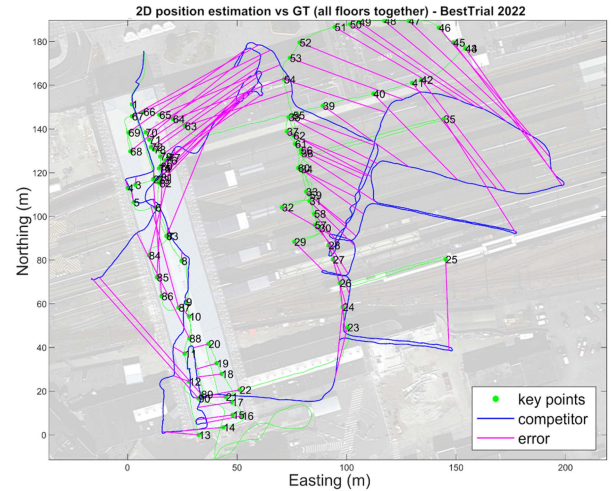


Fig. 39. Trajectory plot of track 4 (2022) best scoring trial.

shared with competitors in a postprocessing mode, was 0.5 m. However, it increased to 62 m in 2021 with EvalAPI in a quasi-real-time mode. Although this can be partly explained by competitors' lack of familiarity with the new platform, the main reason is the causal effect, which does not provide access to future information and makes forward-backward adjustment impossible. Compared with other tracks, track 4 is particularly affected by this effect due to the error accumulation of the inertial sensors. Not many absolute “resets” can be performed on track 4, especially in GNSS-denied environments.

In 2022, a total of five teams chose to compete in track 4. Four teams were able to output quasi-real-time results via the EvalAPI. We note that this is better than the previous edition, both in terms of the number of registered teams and teams able to produce results. As we can see in Fig. 38, the winner achieves an accuracy of about 77 m. Even if it seems worse than the previous editions, a real improvement was achieved taking into account the complexity of the trajectory this year as displayed in Fig. 39. We can see clearly that compared with the ground truth pattern (in green), the competitor's estimated trajectory suffers from a continuous rotation drift, which is typical for the dead reckoning algorithm. The figure shows the best 2-D trace since the introduction of EvalAPI. Its final score of 76.9 m versus 61.9 m for the winner of 2021 is explained by the poor quality of floor estimation that led to 15 m of penalties.

### D. Track 7

In 2021, a total of seven teams provided results for the challenge (see Table IX). Different approaches were investigated by the competitors: three teams relied on LOS-error mitigation approaches, three relied on PFs, and one on a C-SLAM approach. Due to the environment changes, the PF-based approaches deteriorate heavily in performance from Test 1 to 2, as the models are fitted to the specific environments. The EMI-based approaches do not exhibit this problem, as the environmental conditions stay similar. The same holds for the C-SLAM approach. Team ISCAS and Waves shared the first place with almost identical 75th error

TABLE IX  
75TH PERCENTILE OF THE ABSOLUTE ERROR IN  $m$  FOR THE 2021 TRACK 7 COMPETITION

Team	Affiliation	Test 1	Test 2	Avg.	Type
CUMT	China University of Mining and Technology	0.1531	0.1754	0.1643	Error mitigation (EMI)
IDLab	Ghent University –Internet technology and data science lab	0.1734	1.073	0.6236	Fingerprinting
ISCAS	Institute of Software, Chinese Academy of Science	0.0879	0.0912	0.0896	EMI
YAI	Yuan Ze University, National Ilan University	0.7573	2.650	1.704	FP
SPSC	Technical University Graz	0.1592	0.1597	0.1594	C-SLAM
UT_PS	Twente University	0.4032	0.979	0.6914	FP
Waves	Ghent University — Waves research group	0.0723	0.1059	0.0891	EMI

TABLE X  
75TH PERCENTILE OF THE ABSOLUTE ERROR IN  $m$  FOR THE  
2022 TRACK 7 COMPETITION

Team	Affiliation	Score
WHU	Wuhan University	0.51
IMEC	Ghent University — Waves research group	0.21
ISCAS	Institute of Software, Chinese Academy of Science	0.20
CUMT	China University of Mining and Technology	1.06

percentiles of 0.0896 and 0.0891  $m$  (the error differences are within the accuracy limits of the reference system), while team SPSC took the third place with an average score of 0.1594  $m$  with a very consistent accuracy for both environments, which indicates good generalization properties. In general, the competition is advantageous for EMI approaches. In fact, the high number of anchors provides redundancy high enough that reliance on LOS connections yields sufficient spatial information for accurate tracking. As a consequence, no additional multipath information, which is exploited by the other approaches, is required.

In 2022, a total of four teams provided results for the challenge, as detailed in Table X. Team ISCAS achieved the highest performance with a score of 0.20  $m$ , while team IMEC is very close with a score of 0.21  $m$  so that both teams share the first place. Lower results are achieved by team WHU with a score of 0.51  $m$  and team CUMT 1.06  $m$ . The results show that the change of the agent for data acquisition and inference is feasible, as all competitors achieved reasonable accuracies. Teams ISCAS and IMEC have shown that very high performances can be achieved, which indicates that data-driven algorithms can generalize well to different agents. The deterioration of the results w.r.t. 2021 challenge can be explained by the different agents and the quasi-real-time processing of the data to obtain results with the novel introduction of the EvalAPI.

## XII. LESSONS LEARNED

### A. Lessons Learned by Competitors

#### 1) Track 2—Camera:

a) *Team CamLoc*: Tested many mainstream visual.

Localizing algorithms. Table XI, summarizes their advantages and disadvantages.

#### 2) Track 3—Smartphone:

a) *Team imec-WAVES*: Learned that calculating wall intersections ad hoc for each particle of their PF is very time-consuming. Because of this and the limited time to upload a new position, they could not use many particles. This made it hard

for the PF to recover from mistakes, e.g., turning into the wrong room. However, the reset mechanism worked well, so they still obtained good results. The 3-D graph solved this problem and allowed them to use more particles. In 2022, some new difficulties were introduced: some smartphones did not have a magnetometer and/or barometer, no beacon locations were provided, and the quality of the RSS fingerprints was worse than in 2021. The SmartPDR algorithm relies on the magnetometer and, therefore, the fallback PDR algorithm was not available, thus one of the three trials failed immediately, because of the possibility of a missing barometer and the bad RSS fingerprinting performance, this team could not put confidence in (i.e., gave low weights to) the floor (transition) detection, and the RSS fingerprint matching algorithms. This was a mistake because the path estimation algorithm did not respond to correct floor transition detections and therefore stayed mostly on the same floor.

b) *Team X-LAB*: Identified that the phone used for collecting the data should be fully considered in the fingerprint location process. They also found that it is especially important to prioritize the correctness of each module in the positioning system rather than improving the accuracy of a particular module. An incorrect module will greatly reduce the overall positioning accuracy, just like the barrel effect.

#### 3) Track 6—Smartphone on Vehicle:

a) *Team WHU-GD*: identified that the GNSS raw measurements are important to help determine the GNSS signal quality and that those systems that fuse the GNSS raw measurements and the IMU have potential to provide better accuracy and robustness.

#### 4) Track 7—CIR in Warehouse:

a) *Team imec-WAVES*: Listed their lessons learned as follows.

- 1) Our approach is less suited to agent generalization than environment generalization, which was at the heart of the 2021 IPIN T7 competition. Training data was therefore rather limited and probably contributed to the reduced precision in comparison to last year’s result.
- 2) Attempts to characterize error and ranging reliability based on  $x$  and  $y$  position were not fruitful.
- 3) While successful, the constant velocity PF fails to capture the intricacies of the agent, human, or robotic. The inclusion of higher order terms, a more dynamic approach to the PF motion model or a mixture of models will be investigated in the future.
- 4) No access to future data points for a given timestamp creates problems for reliable motion and angle estimation

TABLE XI  
SUMMARY OF THE MAINSTREAM VISUAL LOCALIZING ALGORITHM

Method	Description	Problem
Structure from Motion	Build a 3-D map with given images, then use PnP to get the pose.	Time-consuming to build and adjust a 3D map; hard to handle the scenarios that never appear in the training set.
Pose Regression	Directly regress the pose with CNN or other neural networks.	Time-consuming to train and adjust a network; hard to generalize to those scenarios that never appear in the training set.
Image Retrieval	Calculate the similarity between query images and images in the database.	Hard to handle the scenarios that never appear in the database.
VO	Use epipolar geometry to infer pose frame by frame.	Need an initial pose; Based on camera coordinate; Drifting.

in the trajectory, as the initial PF is quite noisy. Some predictors have lost their use because of it and were therefore omitted.

- 5) Limited precision of bin timestamps reduced ranging precision; output format should be more carefully checked by organizers.
- 6) Increased fairness and straightforwardness of the online submission platform outweigh the technical hurdles that had to be overcome.

*b) Team SPCSC:* Proposed a model-based method, Bayesian approach, which does not use the provided training data at all. They used parts of the training data to calibrate the anchor positions. Analyzing the results of track 7 of the IPIN 2021 challenge their proposed algorithm compares well to the proposed ML-based approaches, consistently showing robust behavior for all data sets and being only slightly outperformed in terms of accuracy. An important aspect of the methods presented in [50] and [51] is the nonuniform NLOS likelihood, which allows the information contained in multipath to be fused in a soft, Bayesian manner [55], i.e., it constrains the PF-based position estimate using information contained in the NLOS measurements. However, when there is a LOS connection to at least two anchors and these anchors provide enough directional diversity for accurate positioning, the NLOS information has virtually no effect (especially when the mirror sources due to walls in the environment setup are far away). A comparison showed that changing the NLOS likelihood from the proposed nonuniform to a uniform distribution led to no significant difference in the resulting performance metrics. The scenario investigated in track 7 of the IPIN 2021 challenge comprised data of seven anchors. The LOS to every anchor was obstructed over large parts of the trajectory. Due to a large number of anchors, there were only partial obstructed LOS situations, i.e., the LOS to all anchors was never obstructed simultaneously over significant time intervals. Therefore, unlike [50] and [51], the method described in Section IX-D3 does not involve a nonuniform NLOS likelihood. The team assumed that ML-based methods that learn a nonlinear regression model that maps to the agent position  $p_n$  can, in turn, exploit small differences in the imprint of the provided radio signal data, leading to the observed gain in estimation accuracy.

#### 5) Track 8—5G in Open-Plan Office:

*a) Team Mobile:* Proposed an end-to-end solution based on a ML approach. Moreover, they used statistical knowledge to augment data and generate simulated data so that the model could be effectively trained. They believe that if there is more

real data as the training data set, the CatBoost can perform better. However, the current solution does not integrate TOA information well and the trained CatBoost model is unable to cope with the unknown environment.

*b) Team TX8:* Identifies that in Track 8, to realize high-precision positioning, the TAE should be estimated accurately and the outliers caused by the weak LOS paths and NLOS paths must be handled reasonably. They used the RSRP measurements and a path loss model for the TAE estimation. To deal with the outliers in the measurements, the MCC-based EKF was developed. In addition, this team identified that the position and velocity constraints can be used to further reduce positioning error.

### B. Lessons Learned by Track Chairs

1) *Track 3—Smartphone:* Three major lessons learned arose from organising the competition in 2021 and 2022 and the integration with EvalAPI. First, with the integration of real-time assessment, data sampling should be decreased as processing sensors with sampling frequencies of 200 Hz or higher may not allow real-time processing on the competition side. Second, device diversity should be handled carefully as some devices lack the sensors required for positioning or they may behave under expectations. Finally, the location of the anchor seems decisive to avoid the presence of very large errors, while being provided the location of BLE beacons in 2021, no information about the infrastructure was provided in 2022, which drove to unexpectedly high positioning errors.

2) *Track 6—Smartphone on Vehicle:* In track 6 smartphone on-vehicle, four teams were registered and three teams submitted their final results. Two final scores were under 40 m, with the best one at 14.7 m. The key to success appears to be the well-executed combination of vehicle motion constraint information and magnetometer observations including IMU preintegration, ZUPT, NHC, magnetic heading and graph optimization. Considering the long interruptions of GNSS signal in the test data, more to the point is to maintain the vehicle heading accurately.

Considering that more and more mobile phones can support differential positioning, differential positioning results may be provided to improve positioning accuracy. In addition, changing the posture of the mobile phone during the test can be considered, as this is a typical case in a real scenario.

3) *Track 7—CIR in Warehouse:* The presented data are advantageous for EMI approaches because of the high number of available anchors. To allow for a fairer comparison with other approaches, future competitions may feature a lower number of anchors.

### C. Lessons for Competition Organizers

Based on our experience in organizing wide-scale competitions in interesting scenarios, we can provide some insight that can be useful to scholars and organizers of future competitions.

Among good practices in the framework of such competition organization, we may also include: getting information about the site, taking the time to carefully prepare the path and choosing the proper system able to produce your ground truth.

The first two points involve significant time and effort and should be planned well in advance together with trips for on-site surveys and measurements.

The third point, that is producing the ground truth, is a key enabler for any competition. Measuring reference point positions by hand and using a 3-D scan are the two ways used by Track chairs. Advantages of 3-D scans are accuracy, which in 2018 we estimated between 2 and 10 cm [3], [56], and one-shot postprocessing. Disadvantages are being tied to the chosen site if you do not have the skill or the equipment to do the survey yourself, with the risk that your ground truth database will one day or another be known or learnt by future competitors.

### D. Future Direction of the IPIN Competition

Off-site tracks have become more realistic with the introduction of EvalAPI, an interactive, real-time, causal interface, which is intended to emulate a real environment similar to that of on-site tracks.

Challenges ahead are to make the results of on-site and off-site tracks comparable on a regular basis. Ideally, this would involve choosing the same environment for analogous on-site and off-site tracks, as it was done in 2019 for smartphone-based tracks 1 (on-site) and 3 (off-site). At that time, EvalAPI was not available, but this is what was done again in the 2023 edition, for which results are yet to be published.

## XIII. OPEN CHALLENGES AND FUTURE WORK

The IPIN competition has grown in the past years, up to hosting six off-site tracks in 2022. In the last three years, since 2020, it has only hosted off-site tracks, but has started again with on-site tracks in 2023.

The main challenge is to keep it interesting for organizers to dedicate their time to it and for competitors to participate. These two objectives are partially conflicting.

Most organizers are from the academy, and are not funded for their involvement in the competition. Their main interest lies in discussing and experimenting with new ideas, and generally advancing the state of the art in the field. This can be done by adding new tracks, possibly rotating among them from year to year, or by updating the challenges provided by old Tracks.

On the other hand, advancements should not be leaps forward, as this may alienate interest from competitors, which is linked to being able to test and show off their methods and algorithms. For new competitors, this involves being able to learn from past competitions. For recurring competitors, this involves a stable API.

Judging from the continuous and appreciative involvement of organizers, competitors, and the IPIN Conference management, IPIN competitions have so far managed to meet both objectives of novelty and stability, in a delicate balance.

### ACKNOWLEDGMENT

This document presents the experiences of the IPIN competition for 2021 and 2022 editions. All authors listed in this article have either contributed to managing the EvalAPI, organizing the off-site competition tracks, or developing the positioning solutions (competitors).

Track 3 organizers acknowledge Vladimir Bellavista-Parent, Alberto González-Pérez, Filipe Meneses, Maria João Nicolau and Antonio Costa for their invaluable help collecting data.

*Chairmanship:* Francesco Potortì chaired and organized the competition, managed the eval.aaloo.org website containing all the data, and developed/managed the EvalAPI interface software. Antonino Crivello helped with overall management and managed the paper.

*Track 2—Camera:* The team organizing track 2 is composed by Soyeon Lee, B. Vladimirov, and Sangjoon Park.

CamLoc Team (Track 2) is composed by Yushi Chen, Long Wang, Runze Chen, Fang Zhao, Yue Zhuge, and Haiyong Luo.

*Track 3—Smartphone:* The team organizing track 3 is composed by Joaquín Torres-Sospedra, Antoni Perez-Navarro and Antonio R. Jiménez. Fernando J. Alvarez, Fernando J. Aranda, and Felipe Parralejo supported data collection for the 2021 edition. Adriano Moreira, Cristiano Pendão, and Ivo Silva supported data collection for the 2022 edition.

Leviathan Team (Track 3, 2022) is composed by Han Wang and Hengyi Liang.

imec-WAVES Team (Track 3, 2022) is composed by Cedric De Cock and David Plets.

X-LAB Team (Track 3, 2022) is composed by Yan Cui, Zhi Xiong, Xiaodong Li, and Yiming Ding.

*Track 4—Foot-mounted IMU:* The team organizing track 4 is composed by Miguel Ortiz, Ni Zhu, Ziyou Li, and Valerie Renaudin.

X-LAB Team (track 4, 2022) is composed by Yan Cui, Zhi Xiong, Xiaodong Li, and Yiming Ding.

*Track 6—Smartphone on Vehicle:* The team organizing track 6 is composed by Dongyan Wei, Xinchun Ji, and Wenchao Zhang.

WHU-GD Team (track 6, 2022) is composed by Yan Wang, Longyang Ding, Jian Kuang, Xiaobing Zhang, Zhi Dou, and Chaoqun Yang.

*Track 7—CIR in warehouse:* The team organizing track 7 is composed by Sebastian Kram, Maximilian Stahlke, and Christopher Mutschler.

Team imec-WAVES (track 7, 2021) is composed by Sander Coene and Chenglong Li.

Team imec-WAVES (Track 7, 2022) is composed by Sander Coene.

Team SPSC (track 7, 2021) is composed by Alexander Venus, Erik Leitinger, Stefan Tertinek, and Klaus Witrisal.

*Track 8—5G in open-plan office:* The team organizing track 8 is composed by Yi Wang and Shaobo Wang.

Team Mobile (track 8, 2022) is composed by Beihong Jin, Fusang Zhang, Chang Su, Zhi Wang, and Siheng Li.

Team TX8 (track 8, 2022) is composed by Xiaodong Li, Shitao Li, Mengguan Pan, and Wang Zheng.

Team DYS-BUPT (track 8, 2022) is composed by Kai Luo, Ziyao Ma, Yanbiao Gao, Jiaying Chang, Hailong Ren, and Wenfang Guo.

This work was supported in part by the Italian Ministry of Economic Development through the Challenge project under Grant CUP:B89J22002310005; in part by the of MSIT/IITP, Republic of Korea through ICT R&D program, under Grant 2021-0-0124, an augmented reality solution based on visual deep learning with 1-m accuracy for futuristic complex mall; in part by the National Key Research and Development Program under Grant 2020YFB2104200; in part by the National Natural Science Foundation of China under Grant 61872046 and Grant 62261042; in part by the Key Research Projects of the Joint Research Fund for Beijing Natural Science Foundation and the Fengtai Rail Transit Frontier Research Joint Fund under Grant L221003; in part by the Beijing Natural Science Foundation under Grant 4212024 and Grant 4222034; in part by the Strategic Priority Research Program of Chinese Academy of Sciences under Grant XDA28040000; in part by the Key Research and Development Project from Hebei Province under Grant 21310102D; in part by the Fundamental Research Funds for the Central Universities under Grant 2022RC13; in part by the Open Project of the Beijing Key Laboratory of Mobile Computing and Pervasive Device, Institute of Computing Technology, Chinese Academy of Sciences (Track 2, CamLoc); in part by the European Union's Horizon 2020 Research and Innovation programme under the Marie Skłodowska Curie under Grant 101023072 (ORIENTATE: Low-Cost Reliable Indoor Positioning in Smart Factories, <http://orientate.dsi.uminho.pt/>); in part by the Spanish national research projects under Grant PID2021-122642OB-C42, Grant PID2021-122642OB-C43, and Grant PID2021-122642OB-C44; in part by the MCIN/AEI/10.13039/501100011033; in part by the ERDF A way of making Europe in part by the National Key Research and Development Program of China under Grant 2016YFB0502202 (Track 6, Team WHU-GD), and in part by the IMEC cofinanced project UWB-IR AAA (Track 7, Team imec-WAVES).

### Authors' Affiliations

Francesco Potorti and Antonino Crivello are with the Institute of Information Science and Technologies (ISTI) National Research Council of Italy (CNR), 56124 Pisa, Italy (e-mail: potorti@isti.cnr.it; antonino.crivello@isti.cnr.it).

Soyeon Lee, Blagovest Vladimirov, and Sangjoon Park are with the Electronics and Telecommunications Research Institute, Daejeon 34129, South Korea (e-mail: sylee@etri.re.kr; vladimirov@etri.re.kr; sangjoon@etri.re.kr).

Yushi Chen, Long Wang, Runze Chen, and Fang Zhao are with the School of Computer Science (National Pilot Software Engineering School), Beijing University of Posts and Telecommunications, Beijing 100876, China (e-mail: chenryushi@bupt.edu.cn; 92536077@bupt.edu.cn; chenrz925@bupt.edu.cn; zfsse@bupt.edu.cn).

Yue Zhuge and Haiyong Luo are with the Beijing Key Laboratory of Mobile Computing and Pervasive Device, Institute of Computing Technology, Chinese Academy of Sciences, Beijing 100190, China (e-mail: zhugyue21@mails.ucas.ac.cn; yluo@ict.ac.cn).

Antoni Perez-Navarro is with the Faculty of Computer Sciences, Multimedia and Telecommunication, Universitat Oberta de Catalunya, 08035 Barcelona, Spain (e-mail: aperez@uoc.edu).

Antonio R. Jiménez is with the Centre for Automation and Robotics (CSIC-UPM), 28500 Arganda del Rey, Spain (e-mail: antonio.jimenez@csic.es).

Han Wang, Hengyi Liang, Yi Wang, and Shaobo Wang are with the Huawei Technologies Company Ltd., Shenzhen 100015, China (e-mail: wh200720041@gmail.com; hengyiliang2021@gmail.com; yi.wang@huawei.com; shaobo.wang@huawei.com).

Cedric De Cock, David Plets, Sander Coene, and Chenglong Li are with the Department of Information Technology, IMEC-WAVES/Ghent University, 9052 Gent, Belgium (e-mail: cedric.decock@ugent.be; david.plets@ugent.be; sander.coene@ugent.be; chenglong.li@nudt.edu.cn).

Yan Cui, Zhi Xiong, Xiaodong Li, and Yiming Ding are with the College of Automation, Nanjing University of Aeronautics and Astronautics, Nanjing 210016, China (e-mail: cuiyan@nuaa.edu.cn; xiongzhi@nuaa.edu.cn; xiaodongli@nuaa.edu.cn; dingyiming@nuaa.edu.cn).

Fernando Javier Álvarez Franco, Fernando Jesús Aranda Polo, and Felipe Parralejo Rodríguez are with the Sensory System Research Group (GISS), University of Extremadura, 06006 Badajoz, Spain (e-mail: fafranco@unex.es; fer@unex.es; felipe@unex.es).

Adriano Moreira, Ivo Silva, and Joaquin Torres-Sospedra are with the Centro ALGORITMI, Universidade do Minho, 4800-058 Guimarães, Portugal (e-mail: adriano@dsi.uminho.pt; ivo@dsi.uminho.pt; jtorres@algoritmi.uminho.pt).

Cristiano Pendão is with the Department of Engineering, School of Sciences and Technology, University of Trás-os-Montes and Alto Douro, 5000-801 Vila Real, Portugal, and also with the Centro ALGORITMI, Universidade do Minho, 4800-058 Guimarães, Portugal (e-mail: cristianop@utad.pt).

Miguel Ortiz, Xinchun Ji, and Valérie Renaudin are with the GEOLOC Laboratory, AME Department of the University Gustave Eiffel, 44344 Bouguenais, France (e-mail: miguel.ortiz@univ-eiffel.fr; ni.zhu@univ-eiffel.fr; ziyou.li@univ-eiffel.fr; valerie.renaudin@univ-eiffel.fr).

Dongyan Wei, Xinchun Ji, and Wenchao Zhang are with the Aerospace Information Research Institute, Chinese Academy of Sciences, Beijing 100094, China (e-mail: weidy@aircas.ac.cn; jixc@aircas.ac.cn; zhangwenchao@aoc.ac.cn).

Yan Wang, Longyang Ding, and Jian Kuang are with the GNSS Research Center, Wuhan University, Wuhan 430072, China (e-mail: wystem@whu.edu.cn; dingly@whu.edu.cn; kuang@whu.edu.cn).

Xiaobing Zhang, Zhi Dou, and Chaoqun Yang are with the AutoNavi Software Company Ltd., China (e-mail: zxb101266@autonavi.com; milk.coffee.dz@qq.com; markus.ycq@alibaba-inc.com).

Sebastian Kram and Christopher Mutschler are with the Fraunhofer IIS, Fraunhofer Institute for Integrated Circuits IIS, 90411 Nuremberg, Germany (e-mail: sebastian.kram@iis.fraunhofer.de; christopher.mutschler@iis.fraunhofer.de).

Maximilian Stahlke is with the Fraunhofer IIS, Fraunhofer Institute for Integrated Circuits IIS, 90411 Nuremberg, Germany, and also with the Friedrich-Alexander-University Erlangen-Nuremberg (FAU), 91058 Erlangen, Germany (e-mail: maximilian.stahlke@iis.fraunhofer.de).

Alexander Venus, Erik Leitinger, Stefan Tertinek, and Klaus Witrisal are with the Christian Doppler Laboratory for Location-Aware Electronic Systems, Graz University of Technology, 8010 Graz, Austria (e-mail: a.venus@tugraz.at; erik.leitinger@tugraz.at; stefan.tertinek@nxp.com; witrisal@tugraz.at).

Beihong Jin, Fusang Zhang, Chang Su, Zhi Wang, and Siheng Li are with the Institute of Software Chinese Academy of Sciences, Beijing 100190, China (e-mail: jbh@otcaix.xiscas.ac.cn; zhangfusang@otcaix.iscas.ac.cn; suchang21@otcaix.iscas.ac.cn; wangzhi20@otcaix.iscas.ac.cn; lisi-heng19@otcaix.iscas.ac.cn).

Xiaodong Li, Shitao Li, Mengguan Pan, and Wang Zheng are with the Pervasive Communication Research Center, Purple Mountain Laboratories, Nanjing 210000, China (e-mail: lixiaodong@pmlabs.com.cn; 220225900@seu.edu.cn; panmengguan@pmlabs.com.cn; zwang@nuaa.edu.cn).

Kai Luo, Ziyao Ma, Yanbiao Gao, Jiaying Chang, Hailong Ren, and Wenfang Guo are with the Beijing University of Posts and Telecommunications, Beijing 100876, China (e-mail: luokai@bupt.edu.cn; mzy123@bupt.edu.cn; yanbiao.gao@bupt.edu.cn; changjiaying@bupt.edu.cn; sans\_bupt@bupt.edu.cn; guowenfang@bupt.edu.cn).

### REFERENCES

- [1] F. Potorti, A. Crivello, and F. Palumbo, "The EvAAL evaluation framework and the IPIN competitions," in *Geographical and Fingerprinting Data to Create Systems for Indoor Positioning and Indoor/Outdoor Navigation*. New York, NY, USA: Elsevier, 2019, pp. 209–224.
- [2] J. Torres-Sospedra et al., "The smartphone-based offline indoor location competition at IPIN 2016: Analysis and future work," *Sensors (Switzerland)*, vol. 17, no. 3, pp. 1–17, 2017.
- [3] V. Renaudin et al., "Evaluating indoor positioning systems in a shopping mall: The lessons learned from the IPIN 2018 competition," *IEEE Access*, vol. 7, pp. 148594–148628, 2019.
- [4] F. Potorti et al., "Off-line evaluation of indoor positioning systems in different scenarios: The experiences from IPIN 2020 competition," *IEEE Sensors J.*, vol. 22, no. 6, pp. 5011–5054, Mar. 2022.
- [5] F. Potorti et al., "The IPIN 2019 indoor localisation competition—description and results," *IEEE Access*, vol. 8, pp. 206674–206718, 2020.

- [6] F. Potortì et al., "Comparing the performance of indoor localization systems through the EvAAL framework," *Sensors*, vol. 17, no. 10, Oct. 2017, Art. no. 2327.
- [7] D. Lymberopoulos, J. Liu, X. Yang, R. R. Choudhury, V. Handziski, and S. Sen, "A realistic evaluation and comparison of indoor location technologies: Experiences and lessons learned," in *Proc. 14th Int. Conf. Inf. Process. Sensor Netw.*, 2015, pp. 178–189.
- [8] D. Lymberopoulos, J. Liu, X. Yang, R. R. Choudhury, S. Sen, and V. Handziski, "Microsoft indoor localization competition: Experiences and lessons learned," *GetMobile: Mobile Comput. Commun.*, vol. 18, no. 4, pp. 24–31, 2015, doi: [10.1145/2721914.2721923](https://doi.org/10.1145/2721914.2721923).
- [9] D. Lymberopoulos and J. Liu, "The microsoft indoor localization competition: Experiences and lessons learned," *IEEE Signal Process. Mag.*, vol. 34, no. 5, pp. 125–140, Sep. 2017.
- [10] M. Ortiz, "ULISS: A smart device for research on indoor/outdoor positioning and navigation methods," 2022. Accessed: Feb. 22, 2024. [Online]. Available: <https://geoloc.univ-gustave-eiffel.fr/en/hardware/geolocation-of-travelers>
- [11] EvAAL, "EvAAL website," 2023. Accessed: Feb. 22, 2024. [Online]. Available: <https://evaal.aaloo.org/>
- [12] "GNU affero general public license version 3 (AGPL-3.0)," Nov. 2016, Accessed: Aug. 23, 2017. [Online]. Available: <https://www.gnu.org/licenses/agpl-3.0.en.html>
- [13] S. Hausler, S. Garg, M. Xu, M. Milford, and T. Fischer, "Patch-netvlad: Multi-scale fusion of locally-global descriptors for place recognition," in *Proc. IEEE/CVF Conf. Comput. Vis. Pattern Recognit.*, 2021, pp. 14141–14152.
- [14] D. DeTone, T. Malisiewicz, and A. Rabinovich, "Superpoint: Self-supervised interest point detection and description," in *Proc. IEEE Conf. Comput. Vis. Pattern Recognit. Workshops*, 2018, pp. 224–236.
- [15] P.-E. Sarlin, D. DeTone, T. Malisiewicz, and A. Rabinovich, "SuperGlue: Learning feature matching with graph neural networks," in *Proc. IEEE/CVF Conf. Comput. Vis. Pattern Recognit.*, 2020, pp. 4938–4947.
- [16] J. Torres-Sospedra, A. Jiménez, A. Moreira, and E. Al., "Off-line evaluation of mobile-centric indoor positioning systems: The experiences from the 2017 IPIN competition," *Sensors*, vol. 18, no. 2, 2018, Art. no. 487.
- [17] A. R. Jiménez, F. Seco, and J. Torres-Sospedra, "Tools for smartphone multi-sensor data registration and GT mapping for positioning applications," in *Proc. Int. Conf. Indoor Positioning Indoor Navigation*, 2019, pp. 1–8.
- [18] J. D. Gutiérrez et al., "Getsensordata: An extensible android-based application for multi-sensor data registration," *SoftwareX*, vol. 19, 2022, Art. no. 101186. [Online]. Available: <https://www.sciencedirect.com/science/article/pii/S2352711022001121>
- [19] J. Torres-Sospedra et al., "Datasets and supporting materials for the IPIN 2021 competition track 3 (smartphone-based, off-site)," 2021. Accessed: Feb. 22, 2024. [Online]. Available: <https://doi.org/10.5281/zenodo.5948678>
- [20] J. Torres-Sospedra et al., "Datasets and supporting materials for the IPIN 2022 competition track 3 (smartphone-based, off-site)," 2022. [Online]. Available: <https://doi.org/10.5281/zenodo.7612915>
- [21] J. Torres-Sospedra, D. Quezada-Gaibor, A. R. Jiménez, F. Seco, and A. Perez-Navarro, "Datasets and supporting materials for the IPIN 2020 competition track 3 (smartphone-based, off-site)," Zenodo, 2020, doi: [10.5281/zenodo.4314992](https://doi.org/10.5281/zenodo.4314992).
- [22] A. R. Jiménez et al., "Datasets and supporting materials for the IPIN 2019 competition track 3 (smartphone-based, off-site)," 2019, doi: [10.5281/zenodo.3606765](https://doi.org/10.5281/zenodo.3606765).
- [23] A. R. Jiménez et al., "Datasets and supporting materials for the IPIN 2018 competition track 3 (smartphone-based, off-site)," 2018, doi: [10.5281/zenodo.2823964](https://doi.org/10.5281/zenodo.2823964).
- [24] A. R. Jimenez, G. M. Mendoza-Silva, F. Seco, and J. Torres-Sospedra, "Datasets and supporting materials for the IPIN 2017 competition track 3 (smartphone-based, off-site)," 2017, doi: [10.5281/zenodo.2823924](https://doi.org/10.5281/zenodo.2823924).
- [25] A. R. Jimenez, G. M. Mendoza-Silva, R. Montoliu, F. Seco, and J. Torres-Sospedra, "Datasets and supporting materials for the IPIN 2016 competition track 3 (smartphone-based, off-site)," 2016, doi: [10.5281/zenodo.2791530](https://doi.org/10.5281/zenodo.2791530).
- [26] H. Zhang, R. Peng, and X. D. Zhao, "Step detection algorithm using fast Fourier transformation," in *Advanced Materials Research*, vol. 1049. Trans Tech Publ: Gale Academic OneFile, USA, 2014, pp. 1218–1221.
- [27] A. Wang, X. Ou, and B. Wang, "Improved step detection and step length estimation based on pedestrian dead reckoning," in *Proc. IEEE 6th Int. Symp. Electromagn. Compat.*, 2019, pp. 1–4.
- [28] S. Madgwick et al., "An efficient orientation filter for inertial and inertial/magnetic sensor arrays," *Rep. X-IO Univ. Bristol (U.K.)*, vol. 25, pp. 113–118, 2010.
- [29] H. Zou, M. Jin, H. Jiang, L. Xie, and C. J. Spanos, "Winips: WiFi-based non-intrusive indoor positioning system with online radio map construction and adaptation," *IEEE Trans. Wireless Commun.*, vol. 16, no. 12, pp. 8118–8130, Dec. 2017.
- [30] W. Kang and Y. Han, "SmartPDR: Smartphone-based pedestrian dead reckoning for indoor localization," *IEEE Sensors J.*, vol. 15, no. 5, pp. 2906–2916, May 2015.
- [31] N. H. Ho, P. H. Truong, and G. M. Jeong, "Step-detection and adaptive step-length estimation for pedestrian dead-reckoning at various walking speeds using a smartphone," *Sensors (Switzerland)*, vol. 16, no. 9, 2016, Art. no. 1423.
- [32] D. Plets, W. Joseph, K. Vanhecke, E. Tanghe, and L. Martens, "Coverage prediction and optimization algorithms for indoor environments," *EURASIP J. Wireless Commun. Netw.*, vol. 2012, pp. 1–123, 2012.
- [33] B. Li, B. Harvey, and T. Gallagher, "Using barometers to determine the height for indoor positioning," in *Proc. Int. Conf. Indoor Positioning Indoor Navigation*, 2013, pp. 1–7.
- [34] C. Song and J. Wang, "WLAN fingerprint indoor positioning strategy based on implicit crowdsourcing and semi-supervised learning," *ISPRS Int. J. Geo-Inf.*, vol. 6, no. 11, 2017, Art. no. 356.
- [35] C. De Cock, W. Joseph, L. Martens, and D. Plets, "Floor number detection for smartphone-based pedestrian dead reckoning applications," in *Proc. Int. Conf. Indoor Positioning Indoor Navigation*, 2021, pp. 1–6.
- [36] C. De Cock, W. Joseph, L. Martens, J. Trogh, and D. Plets, "Multi-floor indoor pedestrian dead reckoning with a backtracking particle filter and Viterbi-based floor number detection," *Sensors*, vol. 21, no. 13, 2021, Art. no. 4565.
- [37] J. Trogh, D. Plets, L. Martens, and W. Joseph, "Advanced real-time indoor tracking based on the Viterbi algorithm and semantic data," *Int. J. Distrib. Sensor Netw.*, vol. 11, no. 10, 2015, Art. no. 271818.
- [38] M. Ortiz and N. Zhu, "Track4 'Foot-mounted IMU based positioning (off-site)' special features," 2021. Accessed: Feb. 22, 2024. [Online]. Available: [https://evaal.aaloo.org/images/2021/IPIN2021\\_Track4\\_CallForCompetition\\_v2.1.pdf](https://evaal.aaloo.org/images/2021/IPIN2021_Track4_CallForCompetition_v2.1.pdf)
- [39] M. Ortiz and N. Zhu, "Track4 'Foot-Mounted IMU based Positioning (off-site)' results," 2021. Accessed: Feb. 22, 2024. [Online]. Available: [https://evaal.aaloo.org/images/2021/presentations/ipin2021\\_competition\\_track4\\_results.pdf](https://evaal.aaloo.org/images/2021/presentations/ipin2021_competition_track4_results.pdf)
- [40] M. Ortiz and N. Zhu, "Track4 'Foot-Mounted IMU based Positioning (off-site)' special features," 2022. Accessed: Feb. 22, 2024. [Online]. Available: [https://evaal.aaloo.org/files/2022/Track-4\\_TA-2022-v.1.3.pdf](https://evaal.aaloo.org/files/2022/Track-4_TA-2022-v.1.3.pdf)
- [41] M. Ortiz and N. Zhu, "Track4 foot-mounted IMU based positioning (off-site)" results," 2022. Accessed: Feb. 22, 2024. [Online]. Available: <https://evaal.aaloo.org/files/2022/IPIN2022-T4-presentation.pdf>
- [42] X. Li et al., "A pedestrian 3-D position estimation method based on equality constraint and moving platforms correction model," *IEEE Sensors J.*, vol. 22, no. 20, pp. 19596–19607, Oct. 2022.
- [43] A. Molisch, "Ultra-wide-band propagation channels," *Proc. IEEE*, vol. 97, no. 2, pp. 353–371, Feb. 2009.
- [44] H. Wymeersch, S. Marano, W. M. Gifford, and M. Z. Win, "A machine learning approach to ranging error mitigation for UWB localization," *IEEE Trans. Commun.*, vol. 60, no. 6, pp. 1719–1728, Jun. 2012.
- [45] A. Niitsoo, T. Edelhäußer, and C. Mutschler, "Convolutional neural networks for position estimation in TDOA-based locating systems," in *Proc. 9th Intl. Conf. Indoor Positioning Indoor Navigation*, 2018, pp. 1–8.
- [46] C. Gentner, T. Jost, W. Wang, S. Zhang, A. Dammann, and U.-C. Fiebig, "Multipath assisted positioning with simultaneous localization and mapping," *IEEE Trans. Wireless Commun.*, vol. 15, no. 9, pp. 6104–6117, Sep. 2016.
- [47] F. Gustafsson et al., "Particle filters for positioning, navigation, and tracking," *IEEE Trans. Signal Process.*, vol. 50, no. 2, pp. 425–437, Feb. 2002.
- [48] C. Li et al., "Device-free pedestrian tracking using low-cost ultrawideband devices," *IEEE Trans. Instrum. Meas.*, vol. 71, 2022, Art. no. 8501604.
- [49] C. Li et al., "Multistatic UWB radar-based passive human tracking using COTS devices," *IEEE Antennas Wireless Propag. Lett.*, vol. 21, no. 4, pp. 695–699, Apr. 2022.
- [50] A. Venus, E. Leitinger, S. Tertinek, and K. Witrals, "A message passing based adaptive PDA algorithm for robust radio-based localization and tracking," in *Proc. IEEE RadarConf-21*, 2021, pp. 1–6.

- [51] A. Venus, E. Leitinger, S. Tertinek, and K. Witrals, "A graph-based algorithm for robust sequential localization exploiting multipath for obstructed-LOS-bias mitigation," 2022. [Online]. Available: <https://arxiv.org/abs/2207.08646>
- [52] L. Prokhorenkova, G. Gusev, A. Vorobev, A. V. Dorogush, and A. Gulin, "Catboost: Unbiased boosting with categorical features," in *Advances in Neural Information Processing Systems*, S. Bengio, H. Wallach, H. Larochelle, K. Grauman, N. Cesa-Bianchi, and R. Garnett, Eds., vol. 31. Curran Associates, Inc., USA, 2018. [Online]. Available: <https://proceedings.neurips.cc/paper/2018/file/14491b756b3a51daac41c24863285549-Paper.pdf>
- [53] A. Booranawong, K. Sengchuai, D. Buranapanichkit, N. Jindapetch, and H. Saito, "RSSI-based indoor localization using multi-lateration with zone selection and virtual position-based compensation methods," *IEEE Access*, vol. 9, pp. 46223–46239, 2021.
- [54] X. Liu, Z. Ren, H. Lyu, Z. Jiang, P. Ren, and B. Chen, "Linear and nonlinear regression-based maximum correntropy extended Kalman filtering," *IEEE Trans. Syst., Man, Cybern. Syst.*, vol. 51, no. 5, pp. 3093–3102, May 2021.
- [55] S. Mazuelas, A. Conti, J. C. Allen, and M. Z. Win, "Soft range information for network localization," *IEEE Trans. Signal Process.*, vol. 66, no. 12, pp. 3155–3168, Jun. 2018.
- [56] Viametris, 2022. [Online]. Available: <https://viametris.com/>

**Francesco Potorti** (Senior Member, IEEE) received the laurea degree in electronic engineering from University of Pisa, Italy, in 1991.

He is a Senior Researcher with the ISTI-CNR Institute, Pisa, Italy, where he has worked since 1989 in the field of satellite and terrestrial communications until around 2010, when he moved his research interest to indoor localization. He has organized the 2011–2013 EvAAL competitions; defined the EvAAL framework; organised the IPIN competitions from 2014 to 2017; chaired the tenth edition of the IPIN conference in 2019 and the IPIN competitions 2019–2023. He coauthored more than 90 peer-reviewed scientific papers. His current research interests include RSS-based indoor localization, and interoperability and evaluation of indoor localization systems.

Dr. Potorti is a Member of the IPIN Steering Board and is Associate Editor-in-Chief of the IEEE JOURNAL OF INDOOR AND SEAMLESS POSITIONING AND NAVIGATION.



**Antonino Crivello** received the Ph.D. degree in information engineering and science from the University of Siena, Siena, Italy, in 2018.

He is a Researcher with the Information Science and Technology Institute, National Research Council, Pisa, Italy. His research interests include indoor positioning and navigation, with a focus on wireless sensors and neural networks.



**Soyeon Lee** received the B.S. degree in statistics from Ewha Woman's University, Seoul, South Korea, in 1992, the M.S. degree in statistics of computation from Seoul National University, Seoul, in 1994, and the Ph.D. degree in computer and information science from Korea University, Seoul, in 2015.

Since 1994, she has been a Principal Researcher with the Electronics and Telecommunications Research Institute, Daejeon, South Korea. Since 2013, her research topic has been pedestrian dead reckoning focusing on foot-mounted and handheld devices. Since 2016, she has chaired one of the competition tracks in IPIN, Indoor Positioning and Indoor Navigation. Her current research interests include indoor positioning using pedestrian dead reckoning and Bayesian filtering, and human interaction in AR/VR and their military training applications.



**Blagovest Vladimirov** received the B.S. degree in industrial automation from Technical University of Sofia, Sofia, Bulgaria, and the M.E. and Ph.D. degrees in systems engineering from the Nagoya Institute of Technology, Nagoya, Japan.

Since 2010, he has been a Researcher with the Electronics and Telecommunications Research Institute, Daejeon, South Korea. His research interests include machine learning, cognitive systems, and their practical applications.



**Sangjoon Park** received the B.S. and M.S. degrees in electronic engineering from Kyung-Pook National University, Daegu, South Korea, in 1988, and 1990, respectively, and the Ph.D. degree in computer science from North Carolina State University, Raleigh, NC, USA, in 2006.

From 1990 to 2001, he also worked as a Senior Researcher in Agency for Defence Development. Since 2006, he has been the Director of the positioning and navigation technology in Electronics and Telecommunications Research

Institute, Daejeon, South Korea. His current research interests include positioning, wireless sensor network, next generation embedded sensor network, multi sensor data fusion, and target tracking.



**Yushi Chen** received the B.S. degree in software engineering in 2021 from the Beijing University of Posts and Telecommunications, Beijing, China, where he is currently working toward the Ph.D. degree in software engineering.

His research interests include computer vision, simultaneous localization, and mapping.



**Long Wang** received the B.S. degree in software engineering in 2022 from the Beijing University of Posts and Telecommunications, Beijing, China, where he is currently working toward the Ph.D. degree in software engineering at Beijing University of Posts and Telecommunications.

His research interests include computer vision, simultaneous localization, and mapping.



**Runze Chen** (Graduate Student Member, IEEE) received the B.S. degree in software engineering in 2019 from the School of Software Engineering, Beijing University of Posts and Telecommunications, Beijing, China, where he is currently working toward the Ph.D. degree in software engineering.

He is a Visiting Student with the Institute of Computer Technology, Chinese Academy of Sciences, Beijing. His research interests include mobile computing, autonomous vehicles, and

mobile intelligence.



**Fang Zhao** (Member, IEEE) received the B.S. degree in computers and applications from the School of Computer Science and Technology, Huazhong University of Science and Technology, Wuhan, China, in 1990, and the M.S. and Ph.D. degrees in computer science and technology from the Beijing University of Posts and Telecommunications, Beijing, China, in 2004 and 2009, respectively.

She is currently a Professor with the School of Software Engineering, Beijing University of Posts and Telecommunication. Her research interests include mobile computing, location-based services, and computer networks.



**Yue Zhuge** received the B.S. degree in computer science and technology from the Wuhan University of Technology, Wuhan, China, in 2021. She is currently working toward the M.S. degree in computer application technology with the University of Chinese Academy of Sciences, Beijing, China.

Her research interests include computer vision, simultaneous localization, and mapping.



**Haiyong Luo** (Member, IEEE) received the B.S. degree in information engineering from the Department of Electronics and Information Engineering, Huazhong University of Science and Technology, Wuhan, China, in 1989, the M.S. degree in communication and information systems from the School of Information and Communication Engineering, Beijing University of Posts and Telecommunication, Beijing, China, in 2002, and the Ph.D. degree in computer science from the University of Chinese Academy of Sciences, Beijing, in 2008.

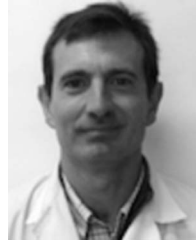
He is currently an Associate Professor with the Institute of Computer Technology, Chinese Academy of Science, Beijing. His main research interests are location-based services, pervasive computing, mobile computing, and Internet of Things.



**Antoni Perez-Navarro** (Member, IEEE) received the bachelor's and Ph.D. degrees in physics from the Universitat Autònoma de Barcelona, Bellaterra, Spain, in 1995 and 2000, respectively.

Between 2017 and 2020, he held the position of Deputy Director of Research with the eLearn Center, Universitat Oberta de Catalunya (UOC) and is Lecturer with the Computer Science, Multimedia, and Telecommunication Department (EIMT Department), since 2005. He is also a Member eHealthLab research group. He is currently the Director of the Technological Observatory with the EIMT department. Apart from his activities at UOC, he works, since the year 2007 with Escola Universitària Salesiana de Sarrià (EUSS). His teaching activities range from the fields of physics and GIS in telecommunication engineering, computer science, multimedia, and industrial engineering. He has authored or coauthored several papers in international journals in all these topics and acts as a reviewer of several journals. His main research interests are indoor positioning, prevention of diseases via smartphones, and e-Learning.

Dr. Perez-Navarro is part of the Technical Program Committee of IPIN and is one of the Chairs of IPIN 2021.



**Antonio Ramón Jiménez** was born in Santander, Spain, in 1968. He received the degree in physics and computer science and the Ph.D. degree in physics from the Universidad Complutense de Madrid, Madrid, Spain, in 1991 and 1998, respectively.

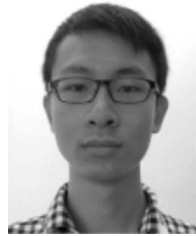
Since 1993, he has been with the Center de Automation y Robotics, Spanish Council for Scientific Research, Madrid, where he holds a research position. He has authored more than 100 articles in journals and conference proceedings. His current research interests include local positioning solutions for indoor/ global positioning system-denied localization and navigation of persons and robots, signal processing, Bayesian estimation, and inertial-ultrasonic-RFID sensor fusion.

Dr. Ruiz is a Reviewer for many international journals and projects in the field.



**Han Wang** (Member, IEEE) received the B.E. and Ph.D. degrees in electrical and electronics engineering from Nanyang Technological University, Singapore, in 2016 and 2021.

Since 2021, he is working as a Research Assistant with the Huawei Technologies, Company Ltd., Shen Zhen, China, where he is currently a Researcher. His research interest, include simultaneous localization and mapping, pedestrian dead reckoning, and computer vision.



**Hengyi Liang** (Member, IEEE) received the B.S. degree in microelectronics from the University of Electronic Science and Technology of China, Chengdu, China, in 2016, and the Ph.D. degree in computer engineering from Northwestern University, Evanston, IL, USA, in 2021.

He is currently a Researcher with Huawei Technologies, Company, Ltd. His research interests include indoor positioning, cyber-physical systems, and connected and autonomous vehicles.



**Cedric De Cock** received the M.S. degree in electronics and ICT Engineering Technology from Ghent University, Ghent, Belgium, in 2020.

In 2020, he became a Member of the imec-WAVES Group, Department of Information Technology, Ghent University. His research interests include IMU-enabled indoor positioning and Bayesian filtering algorithms.



**David Plets** (Member, IEEE) has been a Member of the imec-WAVES Group, Department of Information Technology, Ghent University, Ghent, Belgium, since 2006. He is currently an Associate Professor with the Ghent University. His current research interests include localization techniques and the IoT, for both industry- and health-related applications, and also involved in the optimization of wireless communication and broadcast networks.





**Yan Cui** received the B.S. degree in 2021 from the Nanjing University of Aeronautics and Astronautics, Nanjing, China, where he is currently working toward the master's degree with the Navigation Research Center.

His research interests include indoor inertial navigation and indoor multisource navigation.



**Zhi Xiong** received the M.S. and Ph.D. degrees from the Nanjing University of Aeronautics and Astronautics, Nanjing, China, in 2001 and 2004, respectively.

He joined NUAA, where he has been a Full Professor with the College of Automation, since 2011. In 2013, he was an Academic Visiting Fellow with the University of Southern California, USA. He has ten years' experience in the inertial navigation field and has led more than 30 navigation system development projects. His main

research interests include inertial navigation, small aircraft navigation, brain-like navigation, and multisource fusion.



**Xiaodong Li** received the B.S. degree in automation in 2020 from the Nanjing University of Aeronautics and Astronautics, China, where he is currently working toward the Ph.D. degree with the Department of Automation Engineering.

His research interests include indoor inertial navigation and multisource fusion.



**Yiming Ding** received the M.S. degree from Soochow University, Suzhou, China, in 2018. He is currently working toward the Ph.D. degree with the Navigation Research Center, Nanjing University of Aeronautics and Astronautics, Nanjing, China.

His research interests include pedestrian dead reckoning and wearable sensors.



**Fernando Javier Álvarez Franco** (Senior Member, IEEE) received the M.Sc. degree in physics from the University of Sevilla, Sevilla, Spain, in 1998, the Ph.D. degree in electronics from the University of Alcalá, Alcalá de Henares, Spain, in 2006, the M.Sc. degree in electronic engineering from the University of Extremadura, Badajoz, Spain, in 2012, and the M.Sc. degree in signal theory and communications from the University of Vigo, Vigo, Spain, in 2014.

Since 2001, he has been with the Department of Electrical Engineering, Electronics and Automation, University of Extremadura, where he is currently a Full Professor and the Head of the Sensory Systems Research Group. In 2008, he joined the Intelligent Sensors Laboratory, Yale University, New Haven, CT, USA, as a Post-doctoral "Jose Castillejo" Fellow. His current research interests include local positioning systems, acoustic signal processing, and embedded computing.



**Fernando Jesús Aranda Polo** (Student Member, IEEE) received the B.S. degree in physics from the University of Extremadura, Badajoz, Spain, in 2018, the M.D. degree with a specialization in the simulation of physical phenomena as part of the master's degree in simulation of science and engineering problems with the University of Extremadura, respectively. He is currently working toward the Ph.D. degree with Sensory System Research Group.

Since 2019, he has been a Member of the Sensory System Research Group. His research interests include fingerprinting positioning, machine learning, and radio frequency signal modeling.



**Felipe Parralejo Rodríguez** (Student Member, IEEE) received the B.S. degree in physics and M.D. degree in engineering and science simulation from the Universidad de Extremadura, Badajoz, Spain, in 2019 and 2020, respectively. He is currently working toward the Ph.D. degree with Sensory Systems Research Group, Department of Electrical Engineering and Electronics.

His current research interests include mmWave radar-based human monitoring and the application of machine learning for the processing of the information obtained from intelligent sensors.



**Adriano Moreira** (Senior Member, IEEE) received the degree in electronics and telecommunications engineering and the Ph.D. degree in electrical engineering from the University of Aveiro, Aveiro, Portugal, in 1989 and 1997, respectively.

He is currently an Associate Professor of habilitation with the School of Engineering, University of Minho, Braga, Portugal and a Researcher with Algoritmi Research Centre, Guimarães, Portugal. He is the Director of the MAP-tele Doctoral Program in telecommunications. He has authored more than 100 scientific publications in conferences and journals, and the author of one patent in the area of computational geometry. In the past few years he participated in many research projects funded by national and European programs. His research interests include urban computing, human mobility analysis, indoor positioning and simulation of wireless, mobile networks in urban contexts, and the creation of technologies for smart places.

Dr. Moreira was the recipient of the first prize on the off-site track of the EvAAL-ETRI Indoor Localization Competition (IPIN 2015 and 2017). He is currently the Chair of the Steering Committee of the International Conference on Indoor Positioning and Indoor Navigation and a Member of the ICL-GNSS conference Steering Committee.



**Cristiano Pendão** received the master's degree in telecommunications and informatics from the University of Minho, Braga, Portugal, and the Ph.D. degree in telecommunications/computer science engineering from the University of Minho, University of Aveiro, Aveiro, Portugal, and University of Porto, Porto, Portugal, respectively.

He is currently a Professor with the Department of Engineering, School of Sciences and Technology, University of Trás-os-Montes and

Alto Douro, Vila Real, Portugal. He was a Research Member with ALGORITMI Research Centre, University of Minho. He has coauthored numerous publications in international conferences and journals and has actively participated in several scientific, innovation, and commercial projects within the industry. His research interests include mobile computing, positioning and navigation, computer vision/perception, and machine learning.



**Ivo Silva** received the M.Sc. degree in telecommunications and informatics engineering and the Ph.D. degree (MAP-tele Doctoral Program) in telecommunications from the University of Minho, Minho, Portugal, University of Aveiro, Aveiro, Portugal, and University of Porto, Porto, Portugal, in 2016 and 2022, respectively.

He is a Researcher with Algoritmi Research Centre and an Invited Professor with the University of Minho. He has coauthored several scientific papers in conferences and journals, and

has participated in R&D projects in partnership between academia and industry. His research interests include Industry 4.0, indoor positioning and navigation, vehicle localization, mobile computing, and smart devices.



**Miguel Ortiz** received the M.Sc. degree in mechanics, automation, and engineering from the National School of Arts and Crafts, Meknes, Morocco, in 2001.

He is currently a Research Engineer with GEOLOC Laboratory, University Gustave Eiffel, Bouguenais, France. He joined the lab after six years spent in a company where he managed systems architecture for automotive applications. He is currently an expert in embedded electronic systems. Since 2017, he has been

the Convener of CEN/CENELEC TC5-WG1 named "Navigation and positioning receivers for road applications." Since 2022, he has been the Convener of ISO-TC20-SC14-WG8 named "Downstream space services and space-based applications." He has 15 years of experience in the GNSS domain (research/engineering/standardization). Since 2019, he has been the Deputy Head of GEOLOC Laboratory, Gustave Eiffel University, Bouguenais, France. His research interests include software and hardware developments for both ITS (Intelligent Transport Systems) and pedestrian navigation research field.



**Ni Zhu** (Member, IEEE) received the Engineering degree in aeronautic telecommunications from the National School of Civil Aviation, Toulouse, France, in 2015, and the Ph.D. degree in science of information and communication from the University of Lille, Lille, France, in 2018.

She is currently a Research Fellow with the Laboratory GEOLOC, University Gustave Eiffel, Bouguenais, France. Her research interests include specialization in GNSS channel propagation modeling in urban environments, position-

ing integrity monitoring for terrestrial safety-critical applications, and multisensory fusion techniques for indoor/outdoor pedestrian positioning assisted by artificial intelligence.

Since 2020, she has been the Co-Chair of the foot-mounted IMU-based positioning track of indoor positioning and indoor navigation competition.



**Ziyou Li** received the M.Sc. degree in aerospace navigation and telecommunication from French Civil Aviation University (Ecole Nationale d'Aviation Civile), Toulouse, France, in 2021. He is currently working toward the Ph.D. degree in GNSS pedestrian navigation and integrity monitoring in challenging environments with GEOLOC Laboratory, University Gustave Eiffel, Bouguenais, France.

He joined the GEOLOC Laboratory in 2021.

His research interests include GNSS pedestrian navigation and integrity monitoring in challenging (deep urban and light indoor) environments.

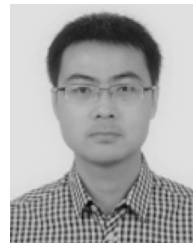


**Valérie Renaudin** (Member, IEEE) received the M.Sc. degree in geomatics engineering and the Ph.D. degree in computer, communication, and information sciences from the Swiss Federal Institute of Technology Lausanne, Lausanne, Switzerland, in 1999 and 2009, respectively.

She is currently a Professor with Gustave Eiffel University, Bouguenais, France. She was the Technical Director with SWISSAT, Schwyz, Switzerland, where she developed real-time positioning solutions based on a permanent global

network of satellite navigation systems (GNSS), and a Senior Research Associate with the University of Calgary, Calgary, AB, Canada. She currently heads the Geopositioning Laboratory, Gustave Eiffel University, where she has built a team specializing in the positioning and navigation of travelers. Her research interests include indoor/outdoor navigation methods and systems using GNSS, as well as inertial and magnetic data, especially for pedestrians to improve sustainable personal mobility.

Dr. Renaudin was the recipient of several awards, including a Marie Curie European Grant for smartWALK project. She founded NAV4YOU, Bouguenais, France, in 2021, developing location-based services for the safety of firefighters in intervention, defence, and underground activities. She is the Editor-in-Chief of the new open access IEEE JOURNAL OF INDOOR AND SEAMLESS POSITIONING AND NAVIGATION that she launched in 2022. She is also a member of the steering committee of the international conference "Indoor Positioning and Indoor Navigation."



**Dongyan Wei** received the B.S. degree in communication engineering from the University of Electronic Science and Technology of China, Beijing, China, in 2006, and the Ph.D. degree in signal and information processing from the Beijing University of Post and Telecommunication, Beijing, in 2011.

He is currently a Research Fellow with Aerospace Information Research Institute, Chinese Academy of Science, Beijing, China. He has authored one book, more than 30 articles,

and more than 20 inventions. His research interests include indoor position, multisensor fusion and positing in wireless network.

Dr. Wei is the TPC Member of IPIN 2019 and the Deputy Chair of IPIN 2022.



**Xinchun Ji** received the B.S. and M.S. degrees in guidance navigation and control from the Beijing University of Aeronautics and Astronautics, Beijing, China, in 2010 and 2013, respectively. He is currently working toward the Ph.D. degree in electronic information with Northwestern Polytechnical University, Xi'an, China.

He is currently an Engineer with Aero Information Research Institute, Chinese Academy of Science, Beijing. His research interests include multisensor fusion and geomagnetic matching.



**Wenchao Zhang** received the B.S. degree in surveying engineering from the China University of Mining and Technology, Xuzhou, China, in 2013, the M.S. degree in surveying engineering from Information Engineering University, Zhengzhou, in 2016, and the Ph.D. degree in signal and information processing from the University of Chinese Academy of Sciences, Beijing, in 2020.

He is currently an Assistant Researcher with Aero Information Research Institute, Chinese Academy of Science (CAS). His research interests include multi-information fusion method, integrated navigation algorithm, and pedestrian autonomous positioning algorithm.



**Yan Wang** received the B.Eng. degree in chemical engineering and technology and the M.S. degree in computer applied technology from the China University of Mining and Technology, Xuzhou, China, in 2016 and 2019, respectively. He is currently working toward the Ph.D. degree with GNSS Research Center, Wuhan University, Wuhan, China.

His research interests include indoor navigation, sensor fusion algorithm, and computer vision.



**Longyang Ding** received the B.Eng. degree (Hons.) in surveying and mapping engineering in 2022 from Wuhan University, Wuhan, China, where he is currently working toward the M.Eng. degree in navigation, guidance, and control with GNSS Research Center.

His research interests include GNSS/INS integration for land vehicle navigation and mobile robot state estimation.



**Jian Kuang** received the B.Eng. and Ph.D. degrees in geodesy and survey engineering from Wuhan University, Wuhan, China, in 2013 and 2019, respectively.

He is currently a Postdoctoral Fellow with GNSS Research Center, Wuhan University, Wuhan, China. His research interests include inertial navigation, pedestrian navigation, and indoor positioning.

**Xiaobing Zhang** received the B.S. degree in computer science and technology from Peking University, Beijing, China, in 2003.

He is currently a Senior Algorithm Expert with Autonavi Software Company Ltd., Beijing, China. His current research interests include inertial navigation with smartphones and crowdsourcing positioning in GNSS-denied scenarios.

**Zhi Dou** received the B.Eng. degree in electronic information engineering from the Hebei University of Technology, Tianjin, China, in 2014, the Ph.D. degree with the School of Electronic Information Engineering, Tianjin University, China, in 2016.

His current research interests include machine learning and vehicle navigation and positioning with smartphones.

**Chaoqun Yang** received the B.Eng. degree in electronic engineering in 2010 from Tsinghua University, Beijing, China, where he continued to study for the Ph.D. degree in electronic engineering and dropped out in 2018.

His research interests include machine learning and GNSS/inertial fusion.



**Sebastian Kram** received the M.Sc. degree in electrical and communication engineering with FAU Erlangen-Nürnberg, Erlangen, Germany, in 2017.

He then joined the Locating and Communication Systems Department, Fraunhofer IIS, Erlangen, Germany. Since 2020, he has been with the Navigation Group, Chair for Information Technology (Communication Electronics) University of Erlangen-Nuremberg, Erlangen, Germany. His research focuses on radio signal-based positioning using both model- and data-driven methods.



**Maximilian Stahlke** received the master's degree in electronic and mechatronic systems from the Institute of Technology Georg Simon Ohm, Nuremberg, Germany, in 2020.

Since 2020, he has been with the Hybrid Positioning and Information Fusion groupworks, Precise Positioning and Analytics Department, Fraunhofer IIS, Erlangen, Germany. His research interests include hybrid positioning for radio-based localization systems with the focus on model- and data-driven information fusion.



**Christopher Mutschler** received the diploma and Ph.D. degrees in computer science from Friedrich-Alexander-University Erlangen-Nuremberg (FAU), Erlangen, Germany, in 2010 and 2014, respectively.

From 2017 to 2019, he was Head and the Chief Scientist with the Machine Learning and Information Fusion Group. He is currently the Head of the Precise Positioning and Analytics Department with Fraunhofer IIS, Nuremberg, Germany. He simultaneously is part-time Scientific Staff with the FAU, offering courses on machine learning.

His research interests include machine learning and hybrid sensor fusion for radio-based locating systems.



**Sander Coene** received the joint M.Sc. degree in nuclear fusion science and engineering physics from the Universität Stuttgart, Stuttgart, Germany, the Université de Lorraine, Lorraine, France, Universiteit Ghent, Ghent, Belgium, Universidad Complutense de Madrid, Madrid, Spain, and Universidad Carlos III de Madrid, Madrid, in 2016. He is currently working toward the Ph.D. degree in electrical engineering with the Ghent University, Ghent.

After a few years of research in the space industry, he joined the WAVES group of the Department of Information Technology, Ghent University in 2020. His research interests include ultrawideband ranging and localization algorithms for indoor applications.



**Chenglong Li** (Member, IEEE) was born in Nanchong, China, in May 1994. He received the Ph.D. degree in electrical engineering from Ghent University, Ghent, Belgium, in 2022.

From 2018 to 2022, he was a Research Assistant with the Department of Information Technology, Ghent University-imec. He is currently a Lecturer with the College of Electronic Science and Technology, National University of Defense Technology, Changsha, China. His current research interests include positioning and

navigation, wireless sensing, wireless channel modeling, and mobile computing.

Dr. Li was the recipient of the International Union of Radio Science Young Scientist Award and European Microwave Association Student Grant in 2022. He was the shared winner of IPIN Competition 2021 track 7.



**Klaus Witrals** (Member, IEEE) received the Ph.D. degree (cum laude) from the Delft University of Technology, Delft, The Netherlands, in 2002, and the Habilitation from the Graz University of Technology, Graz, Austria, in 2009.

He is currently an Associate Professor with the Signal Processing and Speech Communication Laboratory, Graz University of Technology, and Head of the Christian Doppler Laboratory for Location-aware Electronic Systems. His research interests include signal processing

for wireless communications, propagation channel modeling, and positioning.

Dr. Witrals was an Associate Editor for IEEE COMMUNICATIONS LETTERS. He was the Co-Chair of the TWG “Indoor” of the COST Action IC1004, EWG “Localization and Tracking” of the COST Action CA15104. He was leading Chair of the *IEEE Workshop on Advances in Network Localization and Navigation*, and TPC (Co)-Chair of the *Workshop on Positioning, Navigation and Communication*.



**Alexander Venus** (Student Member, IEEE) received the B.Sc. and Dipl.-Ing. (M.Sc.) degrees (with highest honors) in biomedical engineering and information and communication engineering in 2012 and 2015, respectively, from the Graz University of Technology, where he is currently working toward the Ph.D. degree.

From 2014 to 2019, he was a Research and Development Engineer with Anton Paar GmbH, Graz. He is currently a Project Assistant with the Graz University of Technology. His research inter-

ests include radio-based localization and navigation, stochastic modeling, inference on graphs, and estimation/detection theory.



**Yi Wang** (Senior Member, IEEE) received the M.Sc. and Ph.D. degrees in the information engineering from the Beijing University of Posts and Telecommunications, Beijing, China, in 1997 and 2000, respectively.

He joined Huawei research in 2005 working with 4G and 5G technologies. Since 2017, he has been working on 5G positioning and sensing. He owns 278 published patents and 77 scientific papers. Most patents are declared as ETSI type.

Dr. Wang was the Chair of 5G millimeter-wave group in IMT-2020 promotion group in China during 2013–2018.



**Erik Leitinger** (Member, IEEE) received the Dipl.-Ing. (M.Sc.) and Ph.D. degrees (with highest honors) in electrical engineering from Graz University of Technology, Graz, Austria in 2012 and 2016, respectively.

From 2016 to 2018, he was a Postdoctoral Researcher with the Department of Electrical and Information Technology, Lund University, Lund, Sweden. He is currently a University Assistant with Graz University of Technology. His research interests include inference on graphs,

localization and navigation, multiagent systems, stochastic modeling and estimation of radio channels, and estimation/detection theory.

Dr. Leitinger was the Co-chair of the special session “Synergistic Radar Signal Processing and Tracking” at the IEEE Radar Conference in 2021. He is Co-organizer of the special issue “Graph-Based Localization and Tracking” in the *Journal of Advances in Information Fusion*. He was the recipient of the an Award of Excellence from the Federal Ministry of Science, Research and Economy for his Ph.D. Thesis. He is an Erwin Schrödinger Fellow.



**Shaobo Wang** received the graduation degree from Zhejiang University, Hangzhou, China, in 2000.

From 2000 to 2008, he was responsible for the design of baseband receiver algorithms for the 3G OM'S system. From 2008, he led the R&D work of physical-layer and low-MAC algorithms in GSM, UMTS, LTE, and 5G NR systems, laying a foundation for the competitiveness of Huawei's network products. Since 2017, he has been working as the Chief Engineer

leading 5G Advanced Technology Research. He is a Senior Research Expert in the field of wireless communication air interface system and the Deputy Minister of RAN Research Department, Wireless Network, Huawei.

Dr. Wang is/was the General and/or Program Co-Chair of many international conferences/workshops.



**Stefan Tertinek** received the Dipl.-Ing. degree in electrical engineering from the Graz University of Technology, Graz, Austria, in 2007, and the Ph.D. degree in electrical engineering from University College Dublin, Dublin, Ireland, in 2011.

From 2011 to 2018, he was with Danube Mobile Communications Engineering GmbH and Co KG (majority owned by Intel Austria GmbH), Linz, Austria, as a RF System Engineer involved in research and product development of multiple

generations of cellular RF transceiver and modem platforms. In 2018, he joined NXP Semiconductors Austria GmbH and Co KG as a RF System Architect in the Product Line Secure Car Access, where he works on ultrawideband and bluetooth radio technologies. His research interests include localization, radar, and machine learning.



**Beihong Jin** received the B.S. degree in computer science from Tsinghua University, Tsinghua, China, in 1989, and the M.S. and Ph.D. degrees in computer science from the Institute of Software, Chinese Academy of Sciences, Beijing, China, in 1992 and 1999, respectively.

Since 1992, she has been with the Institute of Software, Chinese Academy of Sciences. She is currently a Full Professor with the Institute of Software, Chinese Academy of Sciences. Her research interests include mobile and pervasive

computing, middleware, and distributed systems.



**Fusang Zhang** received the M.S. and Ph.D. degrees in computer science from the Institute of Software, Chinese Academy of Sciences, Beijing, China, in 2013 and 2017, respectively.

He is currently an Associate Professor with the Institute of Software, Chinese Academy of Sciences. His current research interests include mobile and pervasive computing, ad hoc network, and wireless contactless sensing.



**Chang Su** (Graduate Student Member, IEEE) received the B.S. degree in software engineering from Xiamen University, Xiamen, China. He is currently working toward the M.S. degree in software engineering with the Institute of Software Chinese Academy of Sciences, Beijing, China.



**Zhi Wang** received the B.S. degree in software engineering from Beijing Jiaotong University, Beijing, China. He is currently working toward the Ph.D degree in software engineering with the Institute of Software Chinese Academy of Sciences, Beijing, China.



**Siheng Li** (Student Member, IEEE) received the B.S. degree in software engineering from Xiamen University, Xiamen, China. He is currently working toward the Ph.D. degree in theory and technology of network distributed computing with the Institute of Software, Chinese Academy of Sciences, Beijing, China.



**Xiaodong Li** was born in Henan, China, in 1991. He received the B.S., M.S., and Ph.D. degrees in information and communication engineering from the Harbin Institute of Technology, Harbin, China, in 2014, 2016, and 2020, respectively.

He is currently a Researcher with Purple Mountain Laboratories, Nanjing, China. His current research interests include indoor navigation and positioning, statistical signal processing, multisensor data fusion, and machine learning.



**Shitao Li** is currently working toward the master's degree with Southeast University, Nanjing, China.



**Mengguan Pan** (Member, IEEE) received the B.S. degree in electronics information engineering and Ph.D. degree in signal and information processing from the School of Electronic Engineering, Xidian University, Xi'an, China, in 2013 and 2018, respectively.

He is currently a Researcher with Pervasive Communication Research Center, Purple Mountain Laboratories, Nanjing, China. His research interests include parameter estimation in radar and wireless communication systems, array signal processing, wireless localization, and integrated sensing and communications.



**Wang Zheng** received the Ph.D. degree in communication and information systems from the College of Electronic and Information Engineering, Nanjing University of Aeronautics and Astronautics, Nanjing, China, in 2021.

He is currently with Pervasive Communication Research Center, Purple Mountain Laboratories, Nanjing. His current research interests include angle of arrival estimation, indoor positioning, and sparse array signal processing.



**Kai Luo** received the B.S. degree in electronic engineering and technology from the North China University of Technology, Beijing, China, in 2019. He is currently working toward the Ph.D. degree in electronic science and technology with the Beijing University of Posts and Telecommunications, Beijing.

His current research areas include indoor and outdoor high-precision positioning and navigation, multisource fusion, signal systems, and signal processing.



**Ziyao Ma** received the B.S. degree in communication engineering from the Beijing University of Posts and Telecommunications, Beijing, China, where he is currently working toward the Ph.D. degree in electronic science and technology.

His current research interests include communication and navigation integration, 5G positioning, and 5G signal processing.



**Yanbiao Gao** received the B.S. degree in electronic engineering from Northeastern University, Shenyang, China. He is currently working toward the Ph.D degree in electronic science and technology with the Beijing University of Posts and Telecommunications, Beijing, China.

His current research include PRS positioning and 5G communications.



**Jiaxing Chang** received the B.S. degree in electronic information science and technology from the Beijing University of Posts and Telecommunications, Beijing, China, where he is currently working toward the master's degree in electronic science and technology.

His current research interests include indoor localization and transfer learning.



**Wenfang Guo** received the B.S. degree in electronic and information engineering from the University of South China, Hengyang, China. She is currently working toward the M.S. degree with the Beijing University of Posts and Telecommunications, Beijing, China.

Her current research interests include the areas of wireless positioning and protocol for 5G NR positioning.



**Hailong Ren** received the B.S. degree in mechanical engineering in 2021 from the Beijing University of Posts and Telecommunications, Beijing, China, where he is currently working toward the M.S. degree in electronic information engineering.

His current research interest includes 5G positioning and 5G signal processing.



**Joaquín Torres-Sospedra** received the Ph.D. degree in computer science from Universitat Jaume I, Castelló, Spain, in 2011.

He is now a Senior Researcher with the University of Minho (Guimarães, Portugal), where he works on Indoor positioning and machine learning for industrial applications. He has authored more than 170 articles in journals and conferences, and supervised 16 Master and 6 Ph.D. students.

Dr. Torres-Sospedra is the Chair of the IPIN International Standards Committee and IPIN Smartphone-based offsite Competition.

Open Access funding provided by 'Consiglio Nazionale delle Ricerche-CARI-CARE-ITALY' within the CRUI CARE Agreement